

ISTANBUL TECHNICAL UNIVERSITY ★ GRADUATE SCHOOL

ROLLER BEARING FAULT DETECTION USING ROTARY ENCODER



M.Sc. THESIS

Samet YALDIZ

Department of Mechanical Engineering

Machine Dynamics, Vibrations and Acoustics Programme

JANUARY 2024

ISTANBUL TECHNICAL UNIVERSITY ★ GRADUATE SCHOOL

ROLLER BEARING FAULT DETECTION USING ROTARY ENCODER



M.Sc. THESIS

**Samet YALDIZ
(503191422)**

Department of Mechanical Engineering

Machine Dynamics, Vibrations and Acoustics Programme

Thesis Advisor: Prof. Dr. Kenan Yüce ŞANLITÜRK

JANUARY 2024

İSTANBUL TEKNİK ÜNİVERSİTESİ ★ LİSANSÜSTÜ EĞİTİM ENSTİTÜSÜ

**AÇISAL ENKODER KULLANARAK BİLYALI RULMANLARDA HATA
TESPİTİ**

YÜKSEK LİSANS TEZİ

**Samet YALDIZ
(503191422)**

Makina Mühendisliği Anabilim Dalı

Makine Dinamiği, Titreşim ve Akustik Programı

Tez Danışmanı: Prof. Dr. Kenan Yüce ŞANLITÜRK

OCAK 2024

Samet YALDIZ, a M.Sc. student of ITU Graduate School student ID 503191422, successfully defended the thesis entitled “ROLLER BEARING FAULT DETECTION USING ROTARY ENCODER”, which he prepared after fulfilling the requirements specified in the associated legislations, before the jury whose signatures are below.

Thesis Advisor: **Prof. Dr. Kenan Yüce ŞANLITÜRK**

Istanbul Technical University

Jury Members : **Prof. Dr. Vahit MERMERTAŞ**

Istanbul Technical University

Dr. Egemen TINAR

Arçelik A.Ş.

Date of Submission : 02 January 2024

Date of Defense : 26 January 2024





To my dearist family,



FOREWORD

I would like to express my deepest gratitude to my advisor, Prof. Dr. Kenan Yüce Şanlıtürk, for his continuous support and guidance during the challenging process of this thesis. His work ethic, motivation, and discipline have been great examples for me as an engineer who believes in intrinsic motivation as key to success.

This project was conducted at the Gasoline and Hydrogen System Research and Development Center of Robert Bosch. Therefore, I extend my gratitude to all my colleagues for their continuous support during the project.

Finally, I would like to thank my dearest family and friends for their continuous support and patience during my thesis study. Special thanks go to my dear wife for her invaluable support, patience, and love.

January 2024

Samet YALDIZ
(Mechanical Engineer)

TABLE OF CONTENTS

	<u>Page</u>
FOREWORD	ix
TABLE OF CONTENTS	xi
ABBREVIATIONS	xiii
SYMBOLS	xv
LIST OF TABLES	xvii
LIST OF FIGURES	xix
SUMMARY	xxi
ÖZET	xxiii
1. INTRODUCTION	1
1.1 Problem	3
1.2 Literature Review	4
1.2.1 Encoder signal-based fault detection	4
1.2.2 Signal de-noising methods	7
1.3 Objective and Scope of the Thesis	11
2. THEORY	13
2.1 Introduction	13
2.2 Instantaneous Angular Speed	14
2.2.1 Operating mechanism of an incremental rotary encoder	14
2.2.2 Measurement of instantaneous angular speed	15
2.3 Bearing Fault Frequencies	15
2.4 Envelope Analysis	17
2.4.1 Hilbert transform	18
2.5 Spectral Kurtosis and the Kurtogram	18
2.5.1 Kurtosis	18
2.5.2 Spectral kurtosis	19
2.5.3 Kurtogram	22
2.6 Signal De-noising and Enhancement	24
2.6.1 Singular value decomposition (SVD)	24
2.6.2 Empirical mode decomposition (EMD)	25
3. EXPERIMENTAL STUDY	29
3.1 Description of Test Bench	29
3.2 Measurement Campaign	31
4. SIGNAL PROCESSING AND RESULTS	33
4.1 Spectral Kurtosis and Envelope Analysis Based Method	33
4.2 SVD and EMD Based Method	37
4.3 Fault Detection Method Based on Removal of Deterministic Components	45
5. CONCLUSIONS AND SUGGESTIONS	51
5.1 Conclusions	51
5.2 Suggestions for Future Works	54
REFERENCES	55
CURRICULUM VITAE	61



ABBREVIATIONS

IAS	: Instantaneous Angular Speed
FFT	: Fast Fourier Transform
EEMD	: Ensemble Empirical Mode Decomposition
EMD	: Empirical Mode Decomposition
IAPD	: Instantaneous Angular Phase Demodulation
RMS	: Root Mean Square
IMF	: Intrinsic Mode Function
SNR	: Signal to Noise Ratio
PPR	: Pulses Per Revolution
ADC	: Analog to Digital Converter
BSF	: Ball Spin Frequency
BPFI	: Ball Pass Frequency Inner
BPFO	: Ball Pass Frequency Outer
FTF	: Fundamental Train Frequency
SK	: Spectral Kurtosis
STFT	: Short-Time Fourier Transform
TSA	: Time Synchronous Averaging
IFFT	: Inverse Fourier Transform



SYMBOLS

$\Delta\theta$: Angular distance
N	: Number of encoder slot
ω	: Angular speed
Δt	: Time interval
t	: Time
T	: Sample interval
p	: Number of pulses
f_r	: Shaft speed
α	: Contact angle
n	: Number of rolling elements
d	: Ball diameter
D	: Pitch diameter
ϕ	: Instantaneous phase
σ	: Standard deviation
μ	: Mean deviation
N_w	: Window length
Δf	: Frequency resolution
R	: Rank
ε	: Threshold
σ	: Singular values



LIST OF TABLES

	<u>Page</u>
Table 3.1 : Main characteristic frequencies.....	30





LIST OF FIGURES

	<u>Page</u>
Figure 2.1 : Optical encoder [32].....	14
Figure 2.2 : IAS measurement.....	15
Figure 2.3 : Bearing geometry and impact signal [34].	16
Figure 2.4 : Typical unprocessed and envelope signals originating from localized defects in element bearings [2].	17
Figure 2.5 : Depending on the signal’s distribution, kurtosis values: zero, positive, or negative [40].	19
Figure 2.6 : Calculation of SK for a simulated bearing fault signal (a) Time signal, showing moving time windows. (b) Amplitude of STFT. (c) Spectral kurtosis vs frequency [42]	21
Figure 2.7 : Comparison of (a) the fast kurtogram with (b) the full kurtogram for an impulsive signal from loose parts monitoring [44].....	23
Figure 2.8 : The flowchart of EMD [37].....	28
Figure 3.1 : Schematic presentation of the test bench	29
Figure 3.2 : Front view of the test bench	30
Figure 3.3 : (a) Camshaft, (b) Artificial fault, created on bearing inner ring.....	31
Figure 3.4 : Example measurement	32
Figure 4.1 : Flowchart of applied method in section 4.1	34
Figure 4.2 : Fast kurtogram: (a) M1 fault-free measurement; (b) M2 measurement with 1 mm fault width; (c) M3 measurement with 2 mm fault width.	35
Figure 4.3 : Envelope spectrum of M1 fault-free measurement: (a) band pass filtered with $f_c = 3922.5$ Hz and $bw = 1562.5$ Hz; (b) band pass filtered with $f_c = 18766.3$ Hz and $bw = 12500$ Hz.....	36
Figure 4.4 : Envelope spectrum of M2 and M3 faulty measurements: (a) M2 band pass filtered with $f_c = 3922.5$ Hz and $bw = 1562.5$ Hz; (b) M2 band pass filtered with $f_c = 18766.3$ Hz and $bw = 12500$ Hz; (c) M3 band pass filtered with $f_c = 3922.5$ Hz and $bw = 1562.5$ Hz; (d) M3 band pass filtered with $f_c = 18766.3$ Hz and $bw = 12500$ Hz.....	36
Figure 4.5 : (a) Captured IAS signal from a faulty bearing: M3 measurement, (b) corresponding amplitude spectrum.	37
Figure 4.6 : The first six IMFs of the raw signal.....	38
Figure 4.7 : Raw data EMD applied; amplitude spectrum of first six IMF: (a) IMF1, (b) IMF2, (c) IMF3, (d) IMF4, (e) IMF5, (f) IMF6.....	39
Figure 4.8 : Flowchart of proposed method in section 4.2	40
Figure 4.9 : Normalized singular values of Hankel matrix.....	41
Figure 4.10 : Time waveform of original signal and reconstructed signal: (a) $r = 50$, (b) $r = 350$, (c) $r = 2000$	42
Figure 4.11 : The first 6 IMFs of the de-noised signal.	43
Figure 4.12 : Amplitude spectrums of first three IMF: (a) IMF1, (b) IMF2, (c) IMF3	44
Figure 4.13 : Flowchart of proposed method in section 4.3.....	46

Figure 4.14 : (a) Captured IAS signal from a faulty bearing at 300 rpm: M3 measurement, (b) corresponding amplitude spectrum.....**47**

Figure 4.15 : Amplitude Spectra of filtered IAS signals at: (a) 300 rpm, (b) 400 rpm**48**

Figure 4.16 : Amplitude Spectra of filtered IAS signals at: (a) 600 rpm, (b) 1000 rpm.....**49**

Figure 4.17 : Envelope spectrum of filtered IAS signal at 1000 rpm.**49**



ROLLING BEARING FAULT DETECTION USING ROTARY ENCODER

SUMMARY

For many industrial complex machines, there are various challenging issues which include reducing machine downtime, managing repairs and maximising operating times. Any problem or fault in machines can cause failures and downtimes which in turn can lead to significant economic losses. Therefore, industrial companies need to plan organized maintenance strategies for optimum productivity. Condition based monitoring stands out as a highly effective and dependable method widely utilized in the field of maintenance.

For rotating systems, rolling bearings are one of the commonly used essential machine elements that are prone to unexpected failures. Traditional monitoring methods predominantly rely on conventional vibration measurements. In recent years, a novel approach to monitoring the condition of bearings using torsional vibration signals via encoder has attracted great attention by scholars. Encoder signals offer notable benefits over standard vibration signals. For instance, encoders have higher signal to noise ratio than accelerometers because they are located close to the rotary components while accelerometers suffer from long and complicated transfer paths. Moreover, encoders are usually built-in type sensors which make them part of the available systems, and this brings additional economic advantages for condition monitoring.

However, captured encoder signals are impacted by adverse factors like speed uncertainties due to random load fluctuations and variations in electric supply. These factors predominantly affect low-level signals, where diagnostic information is frequently masked by noise. In order to overcome this challenging problem, researchers continuously strive to create sophisticated signal processing strategies for the effective extraction of crucial diagnostic insights from signals with significant noise interference. In this thesis, conventional and relatively well-established signal processing methods typically employed in vibration-based fault detection are examined and their implementations in encoder-based fault diagnosis are investigated. Particular attention is paid to signal de-noising and enhancement of the measured signals to improve fault detection performance of proposed method.

In the first chapter, the problem addressed in this thesis is introduced in detail and the existing literature is thoroughly reviewed. In the second chapter, encoder specific details and employed signal processing methods are described. Briefly, working principle of encoders and Instantaneous Angular Speed (IAS) measurement concept are examined. Theoretical background of the the signal processing methods used in this thesis are also presented in this chapter.

The subsequent chapter details the experimental setup and outlines the specifics of the measurement campaign. For the experimental part of the study, an existing Bosch test bench, designed for endurance validation of high-pressure pumps, is employed. For the experimental validation of the fault detection methods used in this thesis, artificial faults are created on the inner rings of cylindrical roller bearings. Due to the

complicated design of the setup and the adverse effects encountered during the signal acquisition, measured data inherently contained significant amount of background noise.

Chapter four focuses on the signal processing of the measured raw data, aiming to extract hidden information which is critical for detecting bearing faults. An open-source software, Python, along with its signal processing libraries, are employed to process the measured signal and apply various signal processing methods for extracting diagnostic information from measured data. This software choice is based on the diverse range of available techniques and exponential growth observed in this area. In this chapter, three different methodologies for fault detection are introduced. The first employs envelope analysis and spectral kurtosis for detection of faults on the bearing's inner ring. In this context, different fault sizes are examined, and the effectiveness of a hybrid approach is investigated. The results clearly indicate that successful identification of the fault frequency of the bearing's inner ring can be captured via the envelope spectra. In the second method, signal de-noising is the main focus of the investigation. Empirical mode decomposition and singular value decomposition-based bearing fault detection methodology is proposed and proposed method is compared with direct empirical mode decomposition applied signal without prior signal de-noising. The findings reveal that the proposed methodology effectively identifies the bearing inner ring fault frequency in the presence of considerable amount of background noise. In contrast, approaches relying solely on spectrum analysis and the direct application of empirical mode decomposition demonstrate limited effectiveness under similar conditions. When analyzing instantaneous angular speed variations captured by an encoder, directly detecting fault indicative frequency components is challenging since the bearing fault carries low energy in the signal. Therefore, the third method focuses on removing the most deterministic components from the signal. After filtering, fault frequencies and harmonics were distinguishable in the signal spectra at various speeds, yielding consistent results. Modulation-related sidebands were also observed in the signal. Upon examining the effect of speed, it was found that in our case, detecting bearing frequencies at relatively lower rpms was easier due to the increase in noise content with rising speed. As a result, findings in this thesis leads to the conclusion that encoder signal-based fault detection methods offer an important alternative in bearing condition monitoring. Besides, bearing fault detection capability of the existing methods can be significantly improved by the use of signal de-noising.

ACISAL ENKODER KULLANILAN BİLYALI RULMANLARDA HATA TESPİTİ

ÖZET

Birçok endüstriyel makina için makina duruşlarının azaltılması, bakım süreçlerinin yönetilmesi ve çalışma sürelerinin uzatılması karşılaşılan başlıca zorluklardan birkaçıdır. Makinalarda meydana gelen herhangi bir arıza ya da hata ciddi ekonomik kayıplara sebebiyet verebilecek makina duruşlarına neden olabilir. Bu nedenle endüstriyel şirketler, verimliliklerini optimize edebilmek adına sistematik bir bakım stratejisine ihtiyaç duyarlar. Duruma dayalı bakım stratejisi, verimliliği ve güvenilirliği sayesinde makina bakım alanında en çok kullanılan bakım tekniklerinden biridir.

Rulmanlar dönen sistemlerde yaygın olarak kullanılan temel makina elemanlarından biridir, ancak beklenmedik arızalara eğilimlidirler. Çoğu durum izleme sistemi, geleneksel titreşim ölçümüne dayalıdır. Son yıllarda ise, alternatif bir metodoloji olarak mil açısız titreşimleri temelli rulman hasar tespit yöntemleri araştırmacılar tarafından bir hayli ilgi görmektedir. Öteleme yönündeki titreşimler ile karşılaştırıldığında açısız titreşimlerin kullanılmasının bazı avantajları mevcuttur. Örneğin, enkoderler dönen bileşenlere yakın konumlandıklarından ivmeölçerlerden daha yüksek sinyal-gürültü oranına sahiptir. Ek olarak, açısız enkoderler genellikle mevcut sistemlerin birçoğunda halihazırda bulunan sistemin bir parçası olan dahili tip sensörlerdir. Sisteme genellikle ilave bir sensör eklenmemesi ekonomik avantaj sağlar.

Ancak enkoder sinyalleri düzensiz yük değişimleri ve elektrik sistemindeki dalgalanmalar gibi etmenlerden olumsuz yönde etkilenir ve bu etmenler sinyale gürültü olarak yansır. Tanı bilgisini içeren düşük enerjili sinyallerin gürültü kaynaklı maskelenmesi hata teşhisini zorlaştırır. Bu nedenle araştırmacılar, gürültülü sinyallerden değerli olan tanı bilgilerini çıkarabilmek adına sinyal işleme alanında ileri yöntemler geliştirmek için sürekli çaba sarf etmektedirler. Bu doğrultuda, nispeten kendini kanıtlamış ve geleneksel ivmeölçer bazlı hata tespitinde sık kullanılan yöntemler incelenmiş ve açısız titreşim bazlı hata tespitine uygulanabilirliği araştırılmıştır. İlaveten bu yöntemlerin hibrit kullanılmasına dayalı yeni hata tespit metotları geliştirilmiş ve deneysel doğrulamaları yapılmıştır. Tez kapsamında özellikle sinyal gürültü ayıklama aşamasına ölçüm sinyalinin hata tespit kabiliyetini arttırabilmek adına özel ilgi gösterilmiştir. Sinyal gürültü ayıklanması öncesi ve sonrası durumlar incelenmiş, pozitif yönde katkı yaptığı gözlemlenmiştir.

Tezin ilk kısmında, duruma dayalı bakım stratejileri ve titreşim bazlı uygulamalara kısaca değinildikten sonra ele alınan problem tanımlanmıştır. Problem tanıtımı sonrası mevcut literatür incelenmiştir. Literatür incelemesi enkoder bazlı hata tespit metotları ve sinyal işleme metotları olmak üzere iki alt başlıkta verilmiştir.

İkinci kısımda ise öncelikle anlık açısal hız kavramı ele alınmış, bu başlığın altında enkoder çalışma mekanizması ve mil anlık açısal hız ölçüm metodu tanıtılmıştır. Anlık açısal hız kavramının ele alınması sonrası rulman hata frekansları tanıtılmış, matematiksel alt yapısı ve ilgili formülasyonları verilmiştir. Daha sonra sinyal işlemede kullanılan zarf analizi, spektral kurtosis teknikleri tanıtılmıştır. İlaveten sinyal gürültü ayıklama ve sinyal kalitesinin iyileştirilmesinde kullanılan Tekil Değerlere Ayrıştırma (Singular Value Decomposition, SVD) ve Empirik Mod Ayrıştırma (Empirical Mode Decomposition, EMD) metotlarının teorik alt yapısı özet bir şekilde sunulmuştur.

Takip eden kısımda ise çalışmanın deneysel kısmına odaklanılmış kullanılan test düzeneği tanıtılmış ve ölçüm detayları verilmiştir. Bu çalışma kapsamında Bosch firmasına ait hali hazırda yüksek basınç yakıt pompalarının uzun ömür dayanım testlerinde kullanılan test düzeneği ve ilgili ekipmanlar kullanılmıştır. Test düzeneği içten yanmalı motorlarda kullanılan yakıt enjeksiyon sistemi alt parçası olan yüksek basınç pompasının çalışma koşullarını simüle edecek şekilde tasarlanmıştır. Kullanılan yüksek basınç pompası pistonlu bir pompa olup kam mili vasıtasıyla tahrik edilmektedir. İçten yanmalı motorlardakinin aksine kam mili elektrik motoru vasıtasıyla tahrik edilmekte olup gerekli tork elektrik motoru tarafından karşılanmaktadır. Test düzeneği mekanik sistemlere ilaveten, yakıt ve yağ sistemlerini de içeren hidrolik düzenekler de barındırmaktadır.

Çalışmalar firmaya ait araştırma ve geliştirme departmanın test merkezinde yürütülmüştür. İncelenen metotların deneysel doğrulanması adına sistemde bulunan ve tahrik milini destekleyen rulmanlardan biri hedef seçilmiştir. Seçilen rulman silindirik makaralı rulman olup iç bileziği ayrılabilen ve tekrar sökölüp takılabilmektedir.

Geliştirilen metotların etkinliğini incelemek adına seçilen silindirik makaralı rulmanın iç bileziği üzerinde farklı boyutlarda yapay hatalar oluşturulmuştur. Seçilen rulmanın hatasız ve hatalı olduğu durumları temsilen farklı ölçümler alınmıştır. Bunlardan ilki, rulmanın hatasız olduğu durumda alınan referans ölçüm olarak adlandırılan ölçümdür. İkinci ve üçüncü ölçümler ise 1 mm ve 2 mm hata genişliğine sahip rulmanlar ile alınan hata bilgilerini barındırması beklenen ölçümlerdir. Test düzeneğinin karmaşık yapısı ve ölçüm sırasında karşılaşılan negatif etkenlerden dolayı, ölçülen sinyaller beklendiği üzere önemli ölçüde gürültü içermektedir. Uygulanan sinyal işleme teknikleriyle gürültünün önemli ölçüde ayıklanması ve sinyal kalitesinin iyileştirilmesi hedeflenmektedir.

Dördüncü kısımda, tez kapsamında kullanılan sinyal işleme teknikleri ve metotlar detaylıca incelenmiş, araştırmalar neticesinde elde edilen ulaşılan sonuçlar sunulmuştur. İncelenen sinyallerin analizi ve sinyal işleme metotlarının uygulanması noktasında açık kaynak kodlu bir yazılım olan Python yazılımı ve ilgili sinyal işleme kütüphaneleri kullanılmıştır. Literatür taraması ve araştırmalar esnasında gözlemlenen zengin sinyal işleme teknik çeşitliliği ve exponansiyel büyümeye ithafen Python yazılımı bilinçli olarak tercih edilmiştir.

Dördüncü kısım içerisinde üç ana sinyal işleme metodolojisi sunulmuştur. İlk olarak farklı boyutlarda oluşturulan rulman arızalarını tespit etmek için spektral kurtosis ve zarf analizi tabanlı sinyal işleme metodolojisi kullanılmıştır. Analizler sonucunda rulman iç bilezik arıza frekansı ve harmonikleri zarf spektrumunda başarıyla tespit edilmiştir. Hata genişliği arttırıldığında spektrumlarda görülen rulman iç bilezik hata

frekansı harmoniklerinin deęişimleri incelenmiş, bazı harmoniklerin genliğinin arttığı tespit edilmiştir.

Dördüncü bölümün ikinci kısmında ise tekil deęerlere ayırıştırma ve empirik mod ayırıştırma bazlı rulman hata tespit metodolojisi önerilmiştir. Özellikle tekil deęerlere ayırıştırma sinyal işleme tekniğinde kullanılan matris işlemlerinden kaynaklı görece yüksek bilgisayar performansına gereksinim duyulmaktadır. Bu görece yüksek bilgisayar performansından tasarruf edebilmek adına hedef sinyaller tekrardan örneklenerek veri sayısı düşürülmüştür. Veri sayısının düşürülmesi sonrası sinyalde bulunan gürültünün azaltılması için tekil deęerlere ayırıştırma sinyal işleme tekniğinden faydalanılmıştır. Sinyalde bulunan gürültü ayıklandıktan sonra empirik mode ayırıştırma ile sinyal farklı bantlara ayırıştırılmıştır. Daha sonra ayırıştırılan bu bantlar spektrum analizi vasıtasıyla frekans alanında incelenmiştir. Geliştirilen metot, doğrudan empirik mod ayırıştırma tekniği uygulanan, ön sinyal işleme adımı olarak gürültü ayıklama uygulanmamış sinyal ile kıyaslanmıştır. Elde edilen kıyaslamalar sonucunda, geliştirilen hibrit metot ile rulmanın iç bilezik hata frekansı başarı ile tespit edilebiliyorken, doğrudan spektrum analizi veya sadece empirik mod ayırıştırma tekniğinin uygulanmasıyla rulman hata frekansı tespit edilememiştir.

Anlık açısal hız sinyallerinin doğrudan analizi ile rulman hata tespiti rulman arıza frekanslarının sinyal içerisinde çok düşük bir enerjiye sahip olmasından dolayı bir hayli zorludur. Bu nedenle sinyal içerisinde baskın olan dişli ve mil frekansları gibi kararlı frekansların filtrelenmesi kritik önem arz etmektedir. Bu bağlamda üçüncü metotta sinyal içerisinde yer alan kararlı elemanların filtrelenmesine odaklanılmıştır. Kararlı frekansların filtrelenmesi sonrası genlik ve zarf spektrumlarında filtreleme öncesi tespiti güç olan hata frekansı ve harmonikleri kolaylık ile tespit edilebilmiştir. Ayrıca hatanın dönen bir eleman üzerinde olması dolayısıyla hata frekansının mil dönüş frekansı ile modülasyonu sonucu hata frekansı etrafında yan bantlar gözlemlenmiştir. Alınan ölçümler sadece tek bir hız da alınmamış olup belirli bir hız aralığı taranmıştır. Hız etkisi incelendiğinde ise farklı hızlarda tutarlı sonuçlar elde edildiği görülmüştür. Buna rağmen, mil dönüş hızının artmasıyla gürültü miktarı da arttığı için görece düşük hızlarda rulman iç bilezik arıza frekansı daha kolay tespit edilmiştir.

Sonuç olarak, bu tez kapsamında elde edilen bulgular ışığında, rulmanların mevcut durumlarının izlenmesi ve arızalarının tespiti hususunda enkoder bazlı durum izleme metodlarının, geleneksel ivmeölçer bazlı titreşim metodlarına güçlü bir alternatif olabileceği gösterilmiştir. Bunun yanında, sinyallerden gürültü ayıklanması ile mevcut metodların rulman hata frekansı tespit kabiliyetlerinin önemli ölçüde artırılabilirdiği/artırılabilirdiği gözlemlenmiştir.



1. INTRODUCTION

Machines are designed and manufactured to serve specific purposes within functional requirements of systems during their designed life span. However, unexpected failures can occur due to various reasons such as faulty design, the use of inferior material and incorrect installations etc [1]. These unexpected failures can lead to serious consequences including excessive financial losses in many engineering applications. Therefore, industrial companies need to plan organized maintenance strategies for optimum productivity. The most common one's are shortly explained here.

As the term implies, 'run to break' means that machines operate until the failure of some components or whole machine, no maintenance is carried out. It ensures maximum operating period between shutdowns. For this type of maintenance, cheaper and non-critical machines are well-suited as an example, sewing machines [2]. For preventive-maintenance, activities are scheduled at regular intervals, which are set to occur more frequently than the anticipated failure duration. Maintenance intervals are provided by the supplier of the components according to design criteria. In some instances, parts still might be in good condition although they reach the end of target working period. With this strategy, to be on the safe side, maintenance periods are relatively shorter hence it can lead to consuming excessive spare parts. Lastly, in condition-based maintenance which is also called 'predictive-maintenance', the tasks are performed based on the specific needs of the machine. The possible wears and early signs of faults in a machine are anticipated by means of consistent condition-monitoring, the replacements or repairs can be done when it is needed. Nevertheless, to know a machine's health status, it is necessary to have reliable condition monitoring tools and techniques, and the ability to measure some parameters to assess the machine's health. The process of condition-monitoring involves sensors, signal modifiers, data collection modules, systems and software algorithms for digital signal processing [1]. There are various advantages of the condition-based monitoring over the other techniques. For instance, in long term, it is economic because part repairs or replacements can be planned based on stock status of components. Thus stocks of the

spare parts can be reduced. However, as expected condition-based maintenance has higher initial investment cost in the beginning owing to additional instrumentations as mentioned before. Nonetheless, it is increasingly acknowledged as the most effective maintenance approach across numerous industries. Recent studies indicate a significant growth in the global market value of condition-monitoring over the coming years [2]. This expected increase is largely attributed to the widespread adoption of Industry 4.0 and the development of innovative tools in manufacturing technologies. Condition-based maintenance is anticipated to become an integral component of the 'smart-factory' concept.

Condition-based monitoring focuses on assessing the machine's current status with the goal of forecasting its future state or condition during operation. Obviously, this approach requires gathering sufficient information to assess the health condition of a machine during operation. Two techniques, vibration and oil analyses are more common to gather information about internal conditions of machines.

Some of the other techniques are thermography (temperature analysis), motor current signature analysis, acoustic emission analysis are employed to acquire diagnostic data as well [1].

Vibration analysis is the most preferred techniques due to advantages over other techniques. For instance, in oil analysis method, there's usually a period of at least a few days from the time the samples are gathered to when they are analyzed. On the other hand, in vibration analysis it is possible to acquire the results relatively in short time like couple of hours. Machines without any fault have their normal characteristic vibration signatures under normal operating conditions. Every machine has a specific frequency response characteristic, and this leads a machine to vibrate with certain frequency characteristic. Any mechanical problem or fault in the components leads to changes in vibration characteristics of the machine, more dominantly at characteristic frequencies. With the help of this approach, incipient defects and their location can be detected in machines before they become a critical issue. Different types of vibration can be measured in the machines. One of the most common techniques is based on measuring vibration from machine housing using acceleration transducers. In this method, transducers are mounted on machine casing, preferably, positioned in proximity to bearing that stabilizes the shaft in motion [1]. Measurements can be done in three mutually perpendicular directions. Alternative form of vibration that provides

valuable diagnostic data is torsional vibration. This refers to angular vibration happening along a component's rotational axis. Torsional vibration is characterized by speed variations in different elements and the twisting of a shaft section during the rotation of the machinery. Any mechanical problem or fault in machines causes rotational speed fluctuation on the rotary components. Through the analysis of mentioned fluctuations, the machine's health status and functional capacity can be evaluated, monitored as well [3]. Such fluctuations can be detected using rotary encoders. A rotary encoder's role is to produce a signal that depicts the correlation between angular displacement and time [4]. When compared to vibration-signals, encoder signals offer a number of benefits and can offer a promising solution for condition-based monitoring of various applications [3]. However, encoder signals that are recorded often include measurement noise and can be influenced by disparate components and extraneous vibration sources.

1.1 Problem

Most of the industrial machines present various challenges, such as reducing downtime, managing repairs, and maximizing operating times [5]. Failures or faults in these machines can result in significant downtimes, leading to considerable economic losses. Therefore, it is highly recommended that the conditions of machines should be monitored, and condition-based maintenance strategies should be followed by industrial companies. For rotating machinery, torsional vibration-based condition monitoring of the systems using encoder signal is one of the attractive methods to assess machine's health parameters. However, the encoder signals that are recorded are subject to a range of negative impacts, such as velocity inconsistencies in the system caused by random variations in load and power supply, along with noise from measurements attributed to the inherent noise in amplifier circuits and other similar factors [6]. Low level signals suffer the most from noise sources as the information signals are generally obscured by noise. Consequently, a primary obstacle in condition-monitoring, is extraction of the diagnosis information buried in noisy signals. Recently, numerous sophisticated techniques for vibration-based fault diagnosis have been created. Yet, the performance of these techniques dramatically decreases with significant ambient noise interference in measured signals.

If the noise levels exceed certain limits, fault detection techniques cannot provide expected diagnosis information. Hence, there is a continuing demand for better and more effective techniques to detect various faults in noise affected signals.

1.2 Literature Review

As mentioned earlier, condition-based monitoring and tracking of mechanical systems are crucial for industrial companies, and torsional vibration-based methods are relatively new and promising for the health assessment of mechanical components. In this section, encoder-based fault detection methods and signal de-noising techniques investigated in the existing literature. The main motivation here is that performing a literature survey can yield ideas for possible future works and provide valuable information to researchers who might continue the investigation into signal de-noising and condition-based fault detection.

1.2.1 Encoder signal-based fault detection

Li et al. [4] conducted a review of methods used for measuring angular speed and determined that several are not suitable for measuring Instantaneous Angular Speed (IAS). They introduced two novel approaches utilizing analog-to-digital converter boards and a purely software-based technique for accurate IAS measurement. They emphasize that for an encoder's resolution to effectively capture diverse events linked to a machine's operation and health, it must be notably high. Their research demonstrates that enhancing the accuracy of IAS measurements can substantially improve the effectiveness of IAS based diagnostic methods.

Gu et al. [7] introduced an approach based on the Fast Fourier Transform (FFT) for estimating instantaneous angular speed in noisy environments. Their research focused on how different instantaneous angular speed measurement factors, like encoder's precision and the extent of the signal sequence, influence the results. They discovered that enhanced precision and a more extended signal sequence led to decreased noise in IAS measurements, thereby improving the detection of small IAS variations crucial for early fault detection in condition monitoring. Subsequently, through experimental validation, they showed the efficacy of IAS in identifying issues like the misalignment in adaptable connectors and anomalies in the rotor bar of electric motors. Furthermore,

they contrasted the IAS method with vibration techniques, finding that IAS offers greater acuity in diagnosis of minor faults in motor driven systems compared to vibration analysis.

Renaudin et al. [8] proposed a methodology for bearing condition monitoring that relies on IAS with angular sampling. The method was applied to an automotive gearbox and the front wheel of a small industrial car using both optical and magnetic encoders, with the optical encoders yielding a better quality signal. They examined various types of wear, particularly on the outer and inner ring of bearings, under different conditions such as variable speeds, loads, external forces, gear ratios, and so forth. They employed Fourier transform as a post processing tool. The measurements are revealed considerable differences in magnitudes that correspond to the extent of the fault dimension. The presence of sideband effects was notably observed in cases where the wear occurred on the rotating parts of the bearing, influenced by load modulation.

Zhou et al. [9] introduced an approach for monitoring the condition of feed axis gearboxes using integrated location transducers (encoders), which is based on ensemble empirical mode decomposition. They demonstrated the efficacy of the proposed method in handling nonlinear and nonstationary complex signals via experimental study.

André et al. [5] introduced condition monitoring system for wind turbine using instantaneous angular speed measurement via encoder. They were interested in correcting the perturbations in IAS signals caused by torque and speed variations (non-stationary behaviour). Because the torque and speed variations are the main source of the noise in the spectral observation. To solve mentioned perturbation issue, windowing technique were applied to signal, and encoder resolution reduction effect investigated in order to enable the visibility of the low cyclic frequency phenomena.

Lie et al. [10] developed an advanced fault diagnostic method for the fault identification of a 6-cylinder engine using instantaneous angular speed signal. They used various intelligent algorithm like support vector machine, independent component analysis, EMD. The efficacy is shown using both simulation and experimental data.

Spagnol and Bregant [11] studied on bearing fault detection using IAS signal. Order analysis technique is employed as signal processing technique. They succeeded to detect bearing train defect using IAS.

Roy and Cherevu [12] applied envelope analysis to instantaneous angular speed signal for fault identification. In experimental validation, a gearbox is used. Tests are conducted under varying speeds and loads. One of the important outcomes of this study is that load is an important factor in fault detection, and it requires certain amount of load applied to the system under test. However, it should not be excessive otherwise, it can act as a damper.

Li and Zhang [13] proposed an alternative method for estimating instantaneous angular speed, termed instantaneous angular phase demodulation. They addressed the drawbacks of conventional methods to extended signal sequences, noise from signal digitization, and inherent system noise. They introduced a fault detection procedure based on developed method. Subsequently, they tested this procedure on gearbox under various operational conditions to empirically validate the precision and efficacy of this new instantaneous angular speed measurement and fault detection procedure. Their findings revealed that noise from signal digitization could be notably reduced, even eliminated with their proposed method.

Miao et al. [14] developed an adaptive filtering technique named improved maximum correlated kurtosis deconvolution method to remove noise from encoder signals. To prove effectiveness of the proposed method, experimental study is conducted with a representative wind turbine test rig. Three different cases are investigated through planet gears. Measurement data are acquired from various faulty gears such as root cracked root, corrosion and wear. Performance of the improved technique is compared with comb filtering and latest available deconvolution methods like multipoint optimal minimum entropy deconvolution. It is concluded that their method has superior performance.

Bourdon et al. [15] introduced a signal processing technique designed for diagnosing and assessing the extent of damage in the outer race of taper roller bearings. This approach primarily utilizes a filter operating within the angular domain. They demonstrated that the impact of a defective bearing on rotational speed can be identified through straightforward spectral analysis of instantaneous angular speed,

provided the signal is sampled over a substantial number of points in the angular domain. To evaluate the effectiveness of this newly designed tool, physical tests were conducted on various outer race defects and measurements. In addition, the proposed tool is applied to both stationary and non-stationary signals and the same results are obtained. Further investigation is suggested for inner bearing defect as an extension of this study since modulation effect should be taken into account due to rotation of the shaft.

1.2.2 Signal de-noising methods

Sanliturk and Cakar [16] introduced an innovative approach utilizing singular value decompositions to remove noise from acquired frequency response functions, thereby enhancing quality of collected data. Their method can be applied both frequency response functions and impulse response functions. However, they indicated that impulse response functions show better performance. Developed approach is tested on both numerical and experimental signal and findings are compared. They emphasized the importance of setting an effective rank value to avoid the loss of valuable information.

Wang et al. [17] compared signal de-noising techniques based on wavelet shrinkage threshold, general matching pursuit, and genetic matching pursuit. They tested the methods with both stationary and non-stationary engine noise signals. The methods based on general matching pursuit and genetic matching pursuit were found to be more effective in retaining the high-frequency components while suppressing the low-frequency components of the signals. Furthermore, it was noted that the genetic matching pursuit method could significantly reduce computation time compared to the general matching pursuit method.

Zhao and Ye [18] conducted a comparative analysis of two prevalent signal noise elimination techniques: singular value decomposition and Wavelet transform. While these methods are founded on distinct theoretical bases, they exhibit notably similar signal processing characteristics, especially when the Hankel matrix is employed in singular value decomposition. This similarity is examined in terms of vector space properties and the nature of the Hankel matrix. They applied both methods for simulations and obtained similar results.

A notable distinction, however, is the absence of phase shift in the singular value decomposition signal, unlike the phase lag observed in wavelet decomposition. This difference is highlighted as a key advantage of singular value decomposition over wavelet decomposition.

Abouel-seoud and Elmosry [19] introduced a technique utilizing wavelet transform analysis for diagnosing faults in wind turbines. They evaluated two methods based on wavelet analysis: one using wavelet filtering for noise reduction and the other employing wavelet decomposition for signal smoothing. Their findings suggest that wavelet filtering is more effective for detecting subtle signatures, while wavelet decomposition is better suited for refining smooth signals. Additionally, they developed wavelet-based metrics, including spectrum comparison, spectral kurtosis, and crest factor. These chosen metrics were assessed using artificial defects in gearbox elements, like cracks in planet gear teeth, cracks in the planet carrier, and inner ring cracks in the main bearing. Signals are acquired using torsional vibration monitoring on a planetary gearbox. They identified impulses hidden in noisy signal by wavelet filtering. Their results indicated that Root Mean Square (RMS) value analysis is very promising and good indicator for early fault characterization and detection.

Roy et al. [20] developed a fault diagnosis method utilizing instantaneous angular speed for gearboxes. In their approach, instantaneous angular speed estimation is carried out in the frequency domain. After instantaneous angular speed estimation, time synchronous averaging is implemented on signal to extract periodic part and de-noise the signal. Subsequently, a Fast-Fourier transform is used on the time averaged signal to identify gearbox anomalies. Time synchronous averaging enhances the gear meshing frequency and its sidebands, facilitating easier fault detection. Experimental studies are carried out on four speed gearboxes at different load and speed conditions. These studies found that detecting faults is particularly challenging in a no-load condition, as applying force to the system is necessary. However, the force applied should be moderated to avoid significantly diminishing the gear backlash.

Zhao and Lin [21] proposed an encoder signal-based condition monitoring system for planet gearbox. In the first step, they converted to unprocessed encoder data into a sequence of instantaneous angular accelerations using spectral quadratic weighting. Subsequently, they employed comb filtering (synchronous averaging) to eliminate interference caused by variations in drive and load. Following these steps, they

developed an adaptive noise reduction technique using the Gini coefficient to enhance subtle impulsive signals indicative of defects. In this noise reduction approach, the filter's bandwidth is optimized by maximizing the coefficient value of the signal, rather than relying on a fixed bandwidth. Finally, they implemented the proposed method to simulated and experimental signals in order to detect different kinds of gear defects such as surface spall, tooth crack, debris invasion. They noted that proposed technique provides non-invasive and economical solution for assessing health of rotary devices.

Golafshan and Sanliturk [22] utilized singular value decomposition for signal noise reduction. Hankel matrix is preferred as data matrix. They revealed that noise reduction in the frequency space outperforms that in the time space for identifying faults. It is showed that efficacy of the procedure highly dependent set limit for rank selection. They recommended systematic identification of limit based on kurtosis value of the cleaned signal. Proposed procedure is applied to ball bearings and different type of bearing faults are successfully detected.

Zhao and Jia [23] introduced a signal noise reduction technique based on singular value decomposition, aimed at enhancing faint signal characteristics. In their approach, they used the information-based model contrary to traditional energy-based methods which ignore slight features led by initial defects. They used the periodic modulation intensity as information index to asses informative part of the signal. The method was applied to both simulated and real data concerning two-stage gearbox bearings, proving its capability in extracting faint fault characteristics even amidst substantial noise.

Zhang et al. [24] developed a fault diagnosis method that combines Singular Value Decomposition (SVD) with a radial basis function neural network. They collected experimental data representing fault-free gear and gears with cracks, missing tooth and wear through a specially designed experimental setup. The collected signals were de-noised by SVD, and the energy amount for each frequency range was determined. Subsequently, these calculated values were used as input for the radial basis function neural network training. It is specified that radial basis function neural network is highly efficient and successful for the fault type classification.

Li et al. [25] introduced a novel approach for detecting and diagnosing gear faults through instantaneous angular speed. Their method integrates empirical mode

decomposition with autocorrelation local spectrum for extracting features from a two-stage gearbox. Initially, the signal is reconstructed to address the oversampling problem resulting from the high precision of the angular transducer and the testing speed. Subsequently, the empirical mode decomposition operation is implemented on the signal to derive effective intrinsic mode functions (IMFs). Following this, a cosine similarity index is employed to identify the most responsive IMFs, noting that some may be irrelevant or even misleading. Finally, autocorrelation local spectrum is utilized for noise reduction and feature derivation. Performance of the proposed procedure is validated experimentally with the two different test rigs which were working on different conditions. It is concluded that proposed method is highly effective for gear fault diagnosis.

Xu and Zhao [3] proposed singular spectrum analysis-based method for identifying position variations through linear encoder. This method was employed to isolate faint position changes from the signal. Furthermore, they compared this approach with the Empirical Mode Decomposition (EMD) method. Their findings showed that singular spectrum analysis surpasses EMD in both effectiveness and precision. They tested their approach on the position variability of the slide table in a CNC machine tool, where movement discrepancies were primarily due to the ball screw. Subsequently, they transformed the position signal into a speed signal (IAS) and analyzed it alongside the position variation at different operational speeds. They observed that speed variations were significantly different at various speeds, whereas the position changes remained uniform. They concluded that their proposed method offers a more straightforward physical interpretation compared to fluctuations analyzed through speed.

Yin et al. [26] introduced a noise reduction technique that combines Akaike information criteria and singular value decomposition. For this method, Hankel matrix is selected as trajectory matrix of the signal and its size determined according to the maximum energy of the singular values. In proposed method, Akaike information criteria is employed to determine the number of effective singular values.

To demonstrate the method's efficacy, it is compared with wavelet threshold denoising and empirical mode decomposition enhanced with a Savitky-Golay filter. Additionally, they introduced a 'comprehensive evaluation index' to quantify noise reduction performance. This index includes signal-to-noise ratio, root mean square

error, and waveform correlation index. The procedure was applied to micro vibration signals in reaction wheels for extracting weak harmonic parameters during the pre-processing stage.

Miao et al. [27] proposed a signal de-noising method combining an improved median filter with a wavelet packet approach. The improved median filter is utilized to remove impulse noise from the signal, while wavelet threshold de-noising is employed to eliminate white noise. It was found that the median filter alone is insufficient for complete noise elimination, as it cannot filter out white noise due to the characteristics of the median filter. The efficacy of the developed procedure is confirmed through a combination of simulation and empirical studies.

Miao and Zhao [28] developed a wavelet noise reduction technique that leverages the cyclostationary nature of vibration signals in rotating machinery. This method focuses on retaining stationary and cyclostationary elements while diminishing the impact of random nonstationary components. Unlike conventional approaches, which use multiple data packets as inputs but yield a singular output packet, suggesting some loss of information, this method employs multiple data packets to construct a wavelet transform-based filter for noise elimination. They conducted a comparative analysis between their method and traditional wavelet-based noise reduction techniques. They tested effectiveness of both methods, using a numerical and experimental rubbing fault signal. They showed that their method has better noise elimination performance than the conventional one at all frequency bands.

1.3 Objective and Scope of the Thesis

This thesis primarily aims to develop methodologies based on encoder signals for condition monitoring of bearings. Special focus is placed on the enhancement and de-noising aspects of the measured signals to increase the fault detection performances of the methods studied. The selected methods are experimentally validated using artificial faults, and the efficacy of the developed methods is demonstrated.

The scope of this thesis is outlined as follows:

In the first chapter, an introduction to bearing condition monitoring is presented. Following the introduction, the problem is defined and the literature is reviewed in

order to have a comprehensive insight into the encoder signal-based fault detection and signal de-noising methods.

In the second chapter, instantaneous angular speed and measurement mechanism are described. After that, bearing fault frequencies are presented. Later, some of the common signal processing and de-noising methods are introduced.

The third chapter focuses on the experimental part of the thesis, where the test bench and measurement campaign are described.

In the fourth chapter, the developed signal processing methods are presented and their capability to detect bearing inner ring faults is examined.

The last chapter summarises the main findings and the conclusions of the thesis as well as the suggestions for future work regarding the encoder based roller bearing fault detection and how to further developed the methods presented in this study are given.

2. THEORY

2.1 Introduction

In rotating systems, rolling element bearings play a critical role yet they are vulnerable to unforeseen failures, and they are often the cause of machine breakdowns. Traditional methods operate on the premise that bearing defects manifest as variations in load over time [8, 29]. These variations are associated with impacts that when the rollers traverse the defect area, leading to the stimulation of structural resonances or shifts in shaft positions, detectable as vibrations [30]. One of the classical methods to measure vibration is the use of acceleration transducers. However, this method is sensitive to the transmission line between the source of excitation and the transducer. As a result, its effectiveness may be compromised in situations where vibration damping by the housing is significant. [31]. Recently, an alternative approach to bearing condition monitoring, based on torsional vibration monitoring, has been receiving particular attention from researchers. This approach offers notable advantages over conventional accelerometer-based vibration monitoring. Encoder signals, in particular, demonstrate a superior signal to noise ratio compared to accelerometers owing to their closer placement to rotating elements whereas accelerometers suffer from long and complicated transfer path [3]. Besides, most common accelerometers are only able to reveal vibrations above the lower cut off frequency. This makes accelerometers ineffective for very low speed machine fault detection like wind turbine bearings [3]. On the other hand, encoders are effective in responding to low frequencies and may be utilized across a range of operating speeds. Lastly, encoders are frequently integrated as built-in sensors in systems, thereby offering inherent benefits for comprehensive condition monitoring.

2.2 Instantaneous Angular Speed

2.2.1 Operating mechanism of an incremental rotary encoder

Incremental encoder is a type of transducer that measures speed by transforming angular movement into an electrical output [20]. An optical encoder typically consists of a rotating disc as shown in Figure 2.1 which is installed on the shaft and features evenly distributed gaps. Each set of these gaps alternates between transparent and light-obstructing sections. The rotation of the encoder's disc causes these gaps to intermittently obstruct and allow light to pass to the photodetector, creating a sequence of electrical pulses.

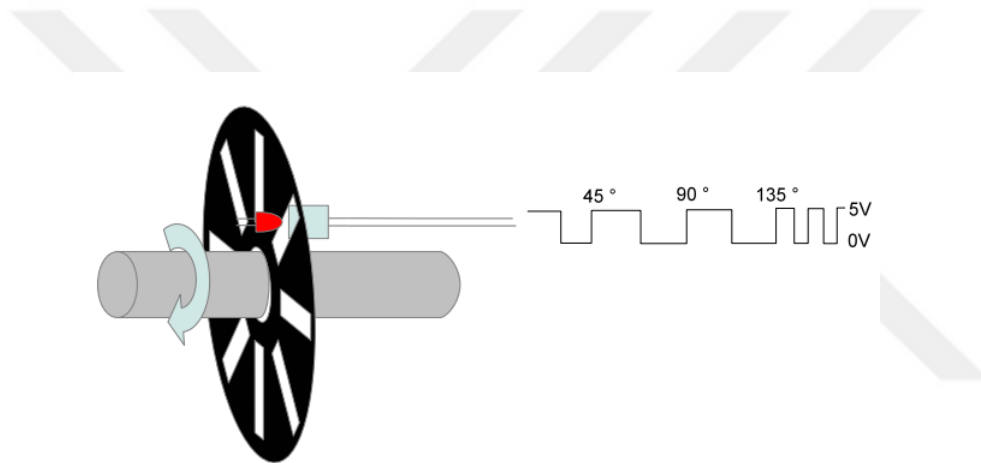


Figure 2.1 : Optical encoder [32]

The resolution of an encoder, which is measured in the amount of pulses per revolution (PPR). It changes according to amount of transparent and light-obstructing sections on the encoder's disk.

The angular displacement $\Delta\theta$ for each equally spaced gap in the disc of the encoder can be written as

$$\Delta\theta = \frac{360^\circ}{N} \quad (2.1)$$

where N represents amount of gap. If it takes Δt time to cover $\Delta\theta$ angle, as a result of its angular speed (ω) for single pulse may be calculated:

$$\omega = \frac{\Delta\theta}{\Delta t} \quad (2.2)$$

2.2.2 Measurement of instantaneous angular speed

Measuring angular velocity is a fundamental task in the surveillance of rotating machinery. A variety of techniques for angular speed measurement have been established. Typically, these techniques fall into two categories: those based on timer-counter mechanisms and those utilizing Analog to Digital Converters (ADC) [4]. The timer-counter-based methods measure the duration between two successive impulses or count the impulses received during sampling interval.

In this study, counter-based method is employed. As a counter, IMC CRONOSflex HRENC-4 module is used. The angular speed calculation method is based on the combination of timing and counting of the impulses. The methodology for calculating angular speed relies on a blend of timing and counting of the impulses. In this method, it is not the time between two pulses that follow one another that is measured, but instead, the time (t) between the first and the last pulse within a sample interval (T) is measured. Angular speed is determined together, with the number of pulses (p) within this sampling interval [5]. The described IAS measurement mechanism is illustrated in Figure 2.2.

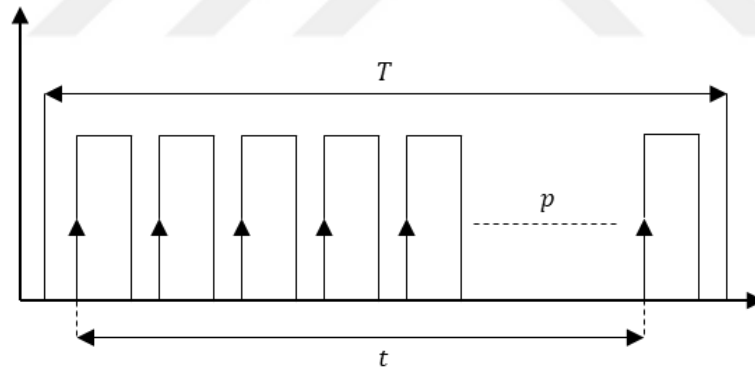


Figure 2.2 : IAS measurement

2.3 Bearing Fault Frequencies

In roller element bearings, an impact occurs when the rolling elements encounter a localized defect on the outer or inner ring, or when a defect on the rolling element itself makes contact with either ring. This impact can trigger high-frequency modes within the structure [2]. These impacts modulate the resonance vibrations and repetition frequencies of the modulations are associated with bearing frequencies such as

Fundamental Train Frequency (FTF), Ball Pass Frequency Outer and Inner race (BPFO, BPFI) and Ball Spin Frequency (BSF), that are formulized as follows [2]:

$$\text{Fundamental train frequency (cage speed): } FTF = \frac{f_r}{2} \left\{ 1 - \frac{d}{D} \cos \alpha \right\} \quad (2.3)$$

$$\text{Ball pass frequency, outer race: } BPFO = \frac{nf_r}{2} \left\{ 1 - \frac{d}{D} \cos \alpha \right\} \quad (2.4)$$

$$\text{Ball pass frequency, inner race: } BPFI = \frac{nf_r}{2} \left\{ 1 + \frac{d}{D} \cos \alpha \right\} \quad (2.5)$$

$$\text{Ball (roller) spin frequency: } BSF = \frac{f_r D}{2d} \left\{ 1 - \left(\frac{d}{D} \cos \alpha \right)^2 \right\} \quad (2.6)$$

Here, f_r represents the rotational speed of the shaft, α is the contact angle between the cage and the ball, n denotes the number of rolling elements, D is the pitch diameter, and d is the diameter of the ball. It should be noted that the frequency of a ball defect is, by its nature, two times of the ball spin frequency since the ball defect impacts both the inner and outer rings in one cycle. Consequently, harmonics of the ball spin frequency are typically prominent in spectrums.

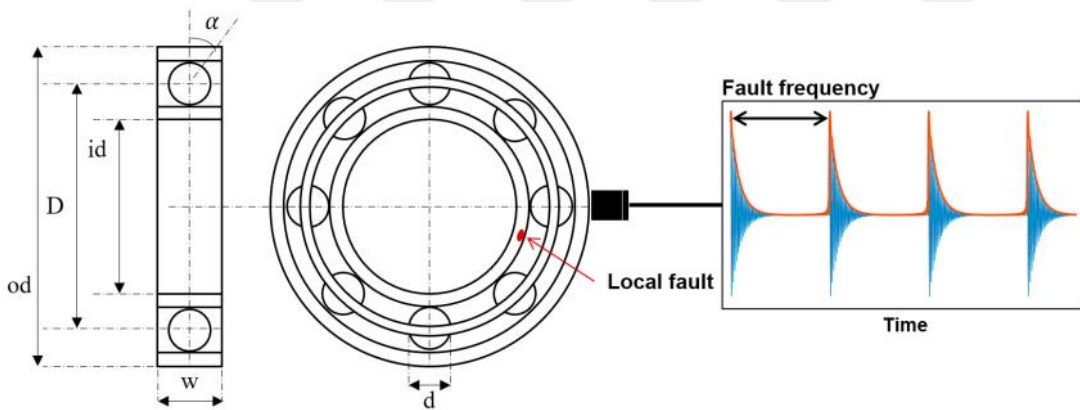


Figure 2.3 : Bearing geometry and impact signal [34].

Frequently, the impact signals corresponding to the defect frequencies influenced by the bearing's higher frequencies. This process generates a periodic signal, similar to an exponentially fading oscillation at the defect frequencies, as shown in Figure 2.3 [34].

2.4 Envelope Analysis

As stated earlier, local faults in roller bearings generates consecutive impacts that can excite some modes of the system. These periodic impacts are modulating the resulting resonance vibrations of the system. As a result of the modulation process, more complex signal arises, and envelope analysis aims to extract the modulating signal from an amplitude-modulated signal. How diagnostic information is obtained using this method is demonstrated below. Figure 2.4 illustrates a typical unprocessed signal and its associated envelope signal.

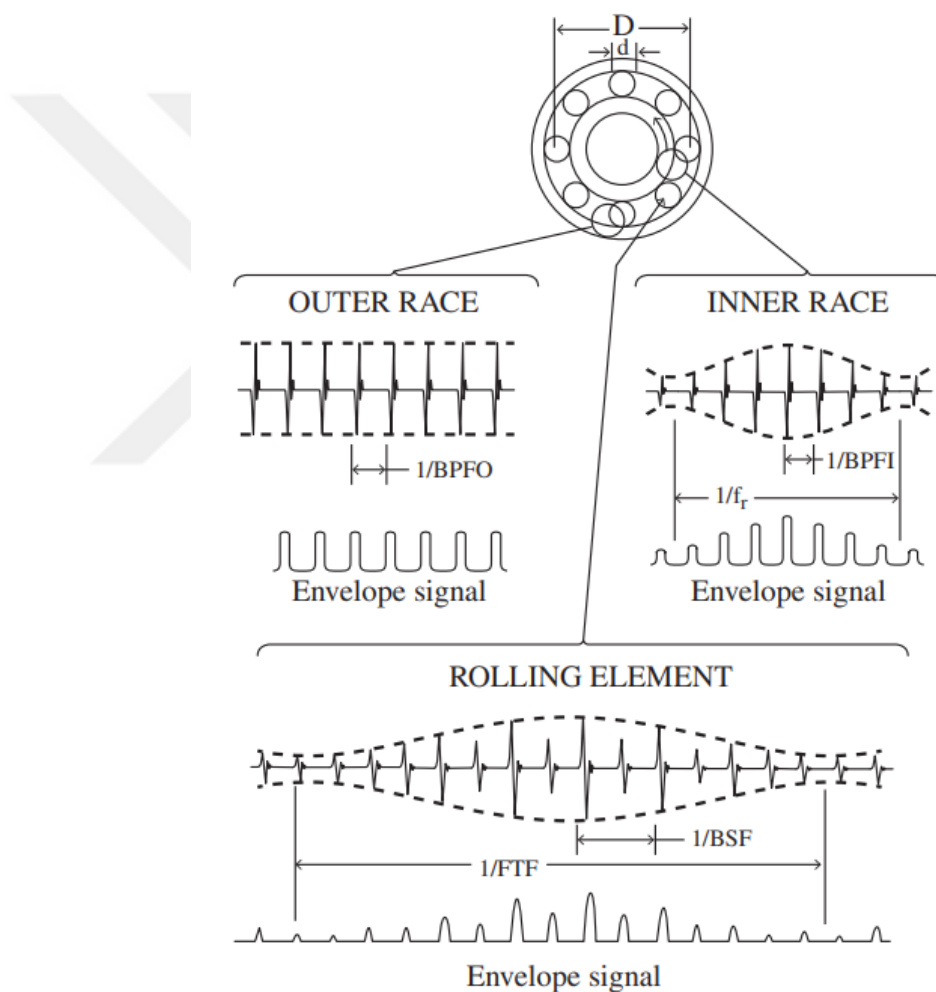


Figure 2.4 : Typical unprocessed and envelope signals originating from localized defects in element bearings [2].

Envelope analysis is one of the powerful and well-established techniques for bearing diagnostic. It enables the demodulation of the signal by separating the fault (envelope) signal from the carrier (resonant) signal through filtering [35]. There are alternative

ways to generate envelope signal. In traditional method, analogue band pass filter plus a rectifier and smoothing circuit are used to perform demodulation [36].

Another popular method in recent years is the use of Hilbert transformation to get the envelope of the time space signal. It produces the envelope by computing the magnitude of the time space function [36].

2.4.1 Hilbert transform

Hilbert transform is also referred to as 90° phase shifter [34] for time domain signals. It results in a signal that is perpendicular in phase to the original input signal, meaning the two signals are positioned at 90 ° to each other in the time-frequency domain [37]. Hilbert transform can be applied to modulated signal to obtain the so-called analytical signal [38]. Analytical signal, in time domain can be represented as follows:

$$A[x(t)] = x(t) + iH[x(t)] = a(t)e^{i\phi(t)} \quad (2.7)$$

$$a(t) = \sqrt{x^2 + H^2[x(t)]} \quad (2.8)$$

$$\phi(t) = \arctan \frac{H[x(t)]}{x(t)} \quad (2.9)$$

where $A[x(t)]$ represents the analytical signal, in which the real part $x(t)$ is the original, measured, amplitude modulated time domain signal, $H[x(t)]$ represents the Hilbert transformation of $x(t)$ and it forms the imaginary part of the analytical signal. $\phi(t)$ notates instantaneous phase and $a(t)$ notates instantaneous amplitude called envelope signal.

2.5 Spectral Kurtosis and the Kurtogram

2.5.1 Kurtosis

Kurtosis is a statistical measure that defines the shape of a signal's distribution in comparison to a Gaussian (normal) distribution, as illustrated in Figure 2.5. Bearings in healthy status exhibit a Gaussian or close to Gaussian distribution, while defected bearings show a non-Gaussian distribution characterized by prominent tails. These tails result from impulses in the signal caused by local defects. As a common metric for assessing the sharpness of a signal's peak, kurtosis effectively indicates signal

impulsiveness, making it a valuable tool for detecting faults in bearings [39]. The definition of kurtosis is as follows:

$$\text{Kurtosis: } (x) = \frac{E\{(x-\mu^4)\}}{\sigma^4} - 3 \quad (2.10)$$

here σ and μ notate the standard deviation and mean of the time series x , whilst $E\{\cdot\}$ is the expectation operator. A standard Gaussian distribution has kurtosis of 3 and is recognized as mesokurtic. Hence, the “minus 3” is appended to the equation's end, ensuring that the kurtosis of a Gaussian distribution equals zero [39].

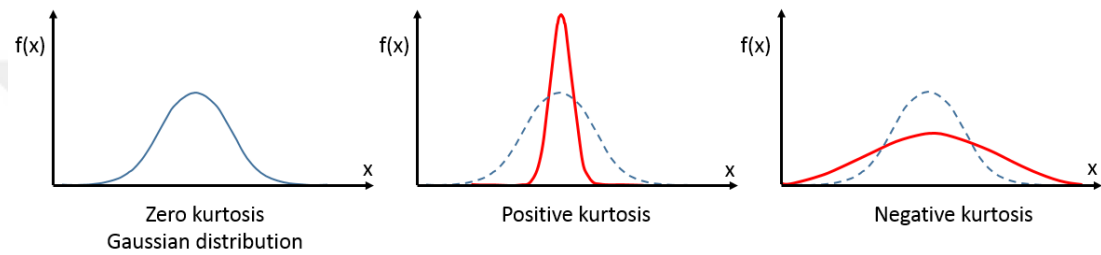


Figure 2.5 : Depending on the signal’s distribution, kurtosis values: zero, positive, or negative [40].

2.5.2 Spectral kurtosis

Basically, as mentioned above, kurtosis is a statistical metrics of the signal which takes highest value in impulsive signals and enables to diagnose bearing faults since faults in rolling elements generate series of impulses when the rolling elements strike on the faulty components. However, vibrations signals are often corrupted by the strong background noises [41]. Therefore, kurtosis is generally not considered as an appropriate global indicator. This makes it necessary to apply kurtosis locally for different frequency bands. Spectral kurtosis concept has been developed to overcome this problem. Spectral Kurtosis (SK) serves as a statistical tool for identifying frequency bands that exhibit impulsive signals [2]. It is particularly useful in pinpointing frequency bands that are predominantly affected by bearing faults [42]. The concept of Spectral Kurtosis was initially introduced in the 1980s for the purpose of identifying impulsive events within sonar signals [2]. Nevertheless, it has not been used effectively for the bearing faults until the Antoni’s studies on the definition and calculations [2]. The concept of Spectral Kurtosis (SK) was originally formulated by Dwyer [42] for stationary signals as the normalized fourth-order moment of the real

part of the short time Fourier transform. Alternatively, Antoni redefined SK using the Wold-Cramer decomposition, making it applicable to both stationary and nonstationary signals.

Here $Y(t)$ output of a causal, linear and time varying system, the Wold-Cramer's decomposition in frequency domain is [39] defined as follows:

$$Y(t) = \int_{-\infty}^{+\infty} e^{i2\pi ft} H(t, f) dX(f) \quad (2.11)$$

where $dX(f)$ is the spectral process associated with $X(t)$ and $H(t, f)$ notates time varying transfer function [43]. It can also be interpreted as complex envelope of vibration signal $Y(t)$ computed by the short time Fourier transform at frequency f and may be defined as follows:

$$H(t, f) = \int_{-\infty}^{+\infty} [x(\tau)\gamma(\tau - t)]e^{-j2\pi ft} dt \quad (2.12)$$

where $\gamma(\tau)$ is a time window function with tiny width.

The normalized fourth-order spectral moment of $Y(t)$ may be specified as:

$$C_{4Y}(f) = S_{4Y}(f) - S_{2Y}^2(f); f \neq 0 \quad (2.13)$$

where $S(f)$ is instantaneous moment of the spectrum, that is used to determine the complex energy and is defined as:

$$S_{2nY}(f) = E\{|H(t, f)dX(f)|^{2n}\}/df \quad (2.14)$$

Antoni [43] advanced the most detailed formulation of Spectral Kurtosis (SK), defining it as the energy balanced fourth order spectral cumulant, indicative of the apex of the probability density function. The SK for an unblemished fault vibration signal $Y(t)$ is characterized as follows:

$$K_Y(f) = \frac{C_{4Y}(f)}{S_{2Y}^2} = \frac{S_{4Y}(f)}{S_{2Y}^2} - 2; f \neq 0 \quad (2.15)$$

As mentioned before, vibration signals often include noise with an unpredictable signal-to-noise ratio. This ratio is defined as the proportion of signal power to noise power and is utilized to gauge the level of ambient noise [39]. This kind of noise

significantly alters the vibration waveform of the signals, obscuring the informative components of the fault signal.

The relationship among the noise $S_Y(f)$, power spectral density of the fault signal $S_M(f)$ and SNR (SNR is also expressed as $1/\rho(f)$), can be expressed as:

$$\rho(f) = \frac{S_M(f)}{S_Y(f)} \quad (2.16)$$

The SK, $K_z(f)$ of the noisy fault vibration signal $Z(t)$ is defined as:

$$K_z(f) = \frac{K_Y(f)}{|1 + \rho(f)|^2} \quad (2.17)$$

From the equation above, it may be deduced that the value of the $K_z(f)$ is close to $K_Y(f)$ at frequencies with low ρ value, where the signal involves diagnostic assets. Hence this interpretation of the equation makes it very special and usable for the optimum band-pass filter design. Another point should be noted that SK calculation results depend on the parameters selected for the STFT. For achieving the maximum kurtosis value, the window length should be set shorter than the interval between individual pulses, yet longer than the duration of each pulse [2]. The described concept is depicted in Figure 2.6.

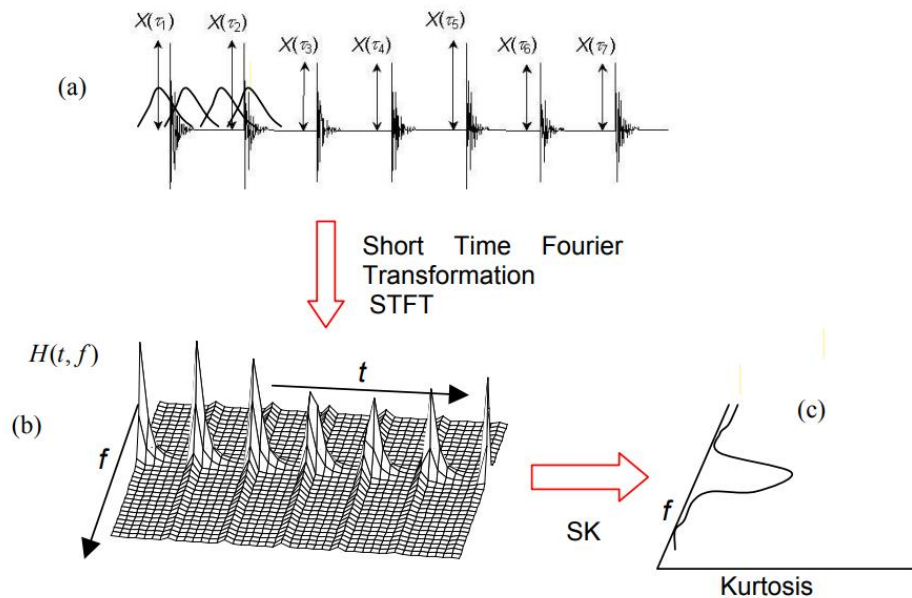


Figure 2.6 : Calculation of SK for a simulated bearing fault signal (a) Time signal, showing moving time windows. (b) Amplitude of STFT. (c) Spectral kurtosis vs frequency [42]

2.5.3 Kurtogram

SK is very useful tool in signal processing, but it is highly dependent to parameter selection. As discussed in the preceding section, the window length (N_w), and consequently the frequency resolution, has a significant impact on the STFT-based SK. Therefore, it is crucial to choose the window length optimally in practical applications. This leads to the pertinent question of how to determine the most suitable frequency resolution (bandwidth) (Δf) for the SK of an arbitrary signal at a specific frequency (f).

Antoni and Randall [44] developed the concept of the kurtogram as a respond to their own question (They preferred to use of frequency resolution instead of bandwidth). The kurtogram, a type of diagram, visually represents the SK values by mapping them in relation to both frequency and frequency resolution. Antoni and Randall [41] proposed the application of a kurtogram for the creation of a band-pass filter, with the objective of maintaining the frequency range that predominantly features the impulsive signals from bearing faults. It means that the optimal frequency and frequency resolution which maximize the SK provides the optimal parameters for the band-pass filter design. Nonetheless, fully investigating the entire spectrum of frequency (f) and frequency resolution (Δf) to determine the exact center frequency and bandwidth is a challenging undertaking, making it less feasible for practical, on the spot industrial use [44]. Therefore, a fast algorithm which is named as ‘fast kurtogram’ was developed by Antoni [44] for the computing of the kurtogram. In this method, consecutive digital filters are used rather than the STFT. Figure 2.7 compares the kurtogram and fast kurtogram of a loose parts monitoring in a nuclear plant [44].

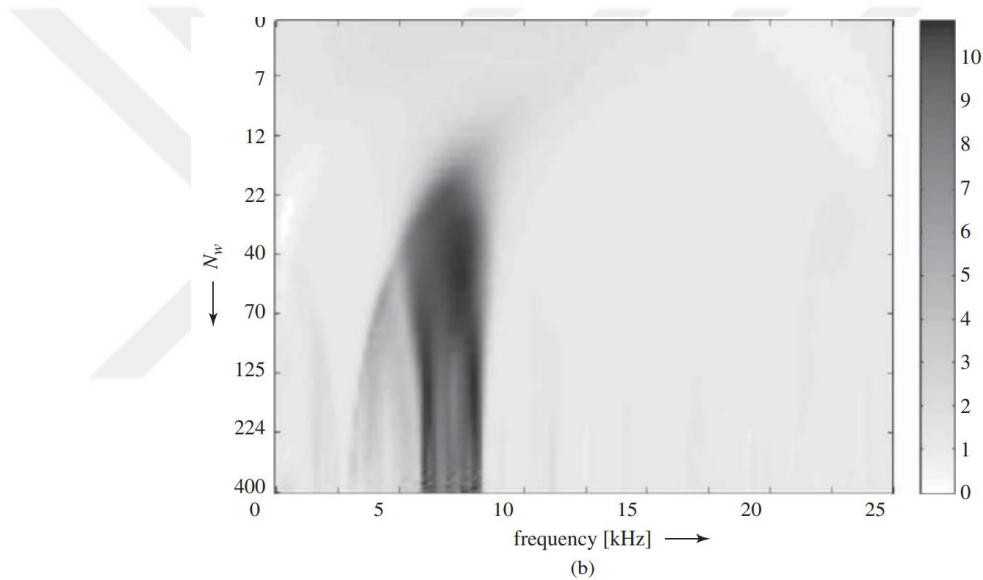
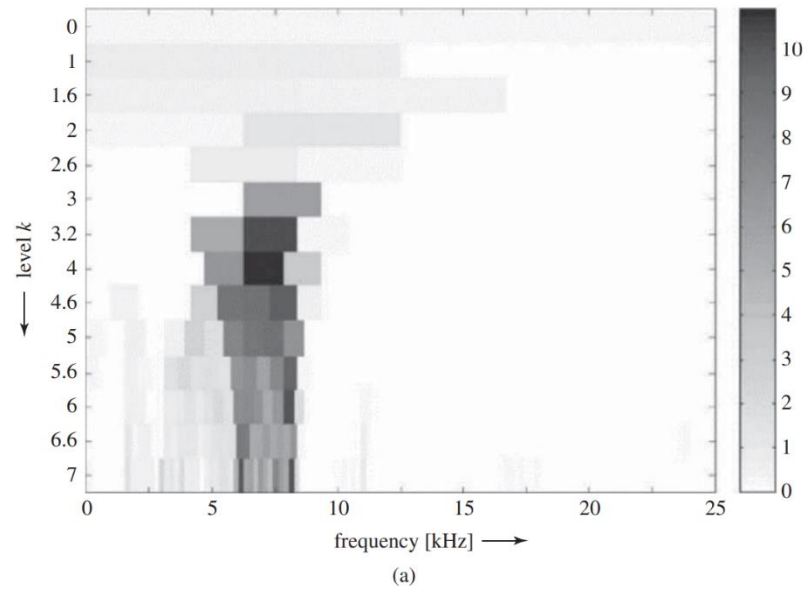


Figure 2.7 : Comparison of (a) the fast kurtogram with (b) the full kurtogram for an impulsive signal from loose parts monitoring [44]

In this particular instance, it is evident that the same selection of center frequency and bandwidth would be used for designing a band-pass filter. The diagram distinctly highlights significant nonstationary activity around the carrier frequency of $f = 6750$ Hz. The frequencies that maximize the kurtosis in this context are the central frequency of 6750 Hz and a frequency resolution of 1500 Hz. These precisely match the frequency band ranging between 6600 and 6900 Hz.

2.6 Signal De-noising and Enhancement

Signal de-noising is a critical aspect of signal processing, aimed at enhancing the quality and reliability of signals by mitigating the influence of unwanted noise. In the context of bearing fault diagnosis and condition monitoring, where signals may be contaminated by various sources of interference, de-noising techniques become indispensable. Within this section, two promising signal cleaning and enhancement method: singular value decomposition and empirical mode decomposition have been introduced.

2.6.1 Singular value decomposition (SVD)

SVD is a computational technique that asserts a matrix $[A]$ can be broken down into the multiplication of three distinct matrices:

$$[A]_{m \times n} = [U]_{m \times m} [S]_{m \times n} [V]_{n \times n}^T \quad (2.18)$$

where $[U]$ is an orthogonal matrix, $[S]$ is a diagonal matrix, and $[V]^T$ is the transpose of an orthogonal matrix $[V]$.

Here $U^T U$ and $V^T V = I$. The matrix S , a diagonal matrix, contains the square roots of the eigenvalues derived from $A^T A$, that can be specified as $S = \text{diag}(\sigma_1, \sigma_1, \dots, \sigma_R)$, where R is the rank of matrix $[A]$ and $R = \min(m, n)$. The terms σ_i (for $i = 1, 2, \dots, L$) are named the singular values of the matrix $[A]$.

$$[S]_{m \times n} = \begin{bmatrix} \sigma_1 & 0 & 0 & 0 & \dots & 0 \\ 0 & \sigma_2 & \dots & 0 & \dots & 0 \\ \dots & \dots & \dots & \dots & \dots & \dots \\ 0 & 0 & \dots & \sigma_r & \dots & 0 \\ \dots & \dots & \dots & \dots & \dots & \dots \\ 0 & 0 & \dots & \dots & \dots & \sigma_n \\ \dots & \dots & \dots & \dots & \dots & \dots \\ 0 & 0 & \dots & 0 & \dots & 0 \end{bmatrix} \quad (2.19)$$

The SVD method is frequently applied in the context of noise elimination, It takes into account a noisy signal vector, denoted as $\{x\} = \{x_0, x_1, x_2, \dots, x_{N-1}\}^T$ comprising N individual samples. This approach is based on the premise that the noise present is additive in nature and exhibits a degree of correlation with the original signal, that is:

$$\{x\} = \{\bar{x}\} + \{ns\} \quad (2.20)$$

where $\{x\}$ notates the signal component and the $\{ns\}$ notatest the noise. Hankel matrix of dimensions $M \times N$ may be created through signal vector $\{x\}$ as [22]

$$[A] = \begin{bmatrix} x_0 & x_1 & \dots & x_{M-1} \\ x_1 & x_2 & \dots & x_M \\ \dots & \dots & \dots & \dots \\ \dots & \dots & \dots & \dots \\ x_{L-1} & \dots & \dots & x_{N-1} \end{bmatrix} \quad (2.21)$$

where $M + L = N + 1$ and $L \geq M$. The signal component within the noisy signal vector is deduced according to the Eckart-Young theorem.

Eckart and Young [45] introduced a method for determining the optimal lower-rank approximation of a given matrix. This method serves as a technique for data reduction, thereby rendering SVD an effective tool for the de-noising of vibration signals. The theorem posits that there is an $m \times n$ matrix $[\bar{A}]$ with a rank $r \leq R$, which minimizes the sum of squared differences between the elements of the original matrix $[A]$ and the corresponding elements in the matrix $[\bar{A}]$. This concept is formulated as

$$[\bar{A}] = [U_r][S_r][U_r]^T \quad (2.22)$$

here $[\bar{A}]$ represents the reconstructed matrix using only the largest number of singular values. Remains are replaced by zero, where ε is threshold.

$$\begin{aligned} \sigma_i &> \varepsilon, i = 1, \dots, r \\ \sigma_i &\leq \varepsilon, i = r + 1, \dots, r \end{aligned} \quad (2.23)$$

2.6.2 Empirical mode decomposition (EMD)

Encoder signals obtained from machinery comprise diverse frequency components resulting from the machine's constituent parts and imbalances within the rotating system. The Empirical Mode Decomposition (EMD) method, which is both thoroughly established and extensively used, facilitates the breakdown of these signals into distinct frequency bands. In this process, EMD breaks down complex signals into Intrinsic Mode Functions (IMFs), which are simpler oscillatory modes that represent natural oscillation frequencies within the signal. This method is particularly effective in analyzing nonlinear and nonstationary signals for fault detection in the field of rotating machinery. According to the EMD criteria, each IMF must independently fulfill the following condition [46]:

- 1) In the whole data set, the number of extremes and the number of zero crossings must either be equal, or only a difference of one is allowed.
- 2) At any point, the mean value of the envelope defined by the local maxima and the envelope defined by the local minima must be equal to zero.

Any raw signal $x(t)$ can be decomposed into intrinsic mode functions using EMD algorithm as follows:

- 1) Identify all the local extremities (both maxima and minima) of the signal and interpolate these points separately using cubic spline lines to create upper and lower envelopes.
- 2) Compute the mean of upper and lower envelope values, labelling this as $m_1(t)$. The difference between $x(t)$ and $m_1(t)$ yields the first component $h_1(t)$, i.e.

$$h_1(t) = x(t) - m_1(t) \quad (2.24)$$

Replace the $x(t)$ by $h_1(t)$, check whether $h_1(t)$, meets the IMF requirements and repeat first two steps until $h_1(t)$ becomes an IMF. Therefore, $c_1(t) = h_1(t)$ is defined as the first IMF.

- 3) Unless $h_1(t)$ is an IMF, it is acted as the input signal and the first two steps are repeated. Then,

$$h_{11}(t) = h_1(t) - m_{11}(t) \quad (2.25)$$

in this process, m_{11} represents the average of the upper and lower envelopes of h_1 . This procedure can be iteratively performed up to k iterations, until h_{1k} qualifies an IMF, that is

$$h_{1k}(t) = h_{1(k-1)}(t) - m_{1k}(t) \quad (2.26)$$

After each shifting processing, it must be checked whether the number of zero crossing equal the number of extreme. If calculated $h_{1k}(t)$ meets the defined conditions, it is regarded as the first IMF as stated below.

$$IMF_1(t) = h_{1k}(t) \quad (2.27)$$

The initial few IMFs correspond to high-frequency events, whereas the latter ones are associated with the low-frequency elements of the signals [46].

4) Subtract IMF_1 from the original signal $x(t)$

$$r_1(t) = x(t) - IMF_1(t) \quad (2.28)$$

Here, r_1 is termed the first residue, encapsulating information about components with longer periods. Subsequently, r_1 is treated as the initial data set, and the sifting process previously prescribed is repeated. This iterative process is capable of being executed n times, enabling the generation of n distinct IMFs components. The outcome of this process is as follows:

$$\left\{ \begin{array}{l} r_1(t) - IMF_2(t) = r_2(t) \\ r_2(t) - IMF_3(t) = r_3(t) \\ \dots \\ r_{n-1}(t) - IMF_n(t) = r_n(t) \end{array} \right\} \quad (2.29)$$

The sifting process persists until it meets the termination criteria for the signal's decomposition. This occurs when the final residual signal, $r_n(t)$, transforms into a monotonic function, beyond any further IMFs can be derived. Alternatively, this endpoint is reached when either the component $IMF_n(t)$ or the residue $r_n(t)$ diminishes to a magnitude deemed negligible.

Finally, the original signal $x(t)$ may be interpreted as a linear superposition of IMFs with a residue $r_n(t)$ based on the EMD algorithm.

$$x(t) = \sum_{i=1}^n IMF_i(t) + r_n(t) \quad (2.30)$$

Here, the IMFs ($IMF_1, IMF_2, IMF_3, \dots, IMF_n$) represent various frequency bands listed from high to low. The flow described above is also visualized in Figure 2.8.

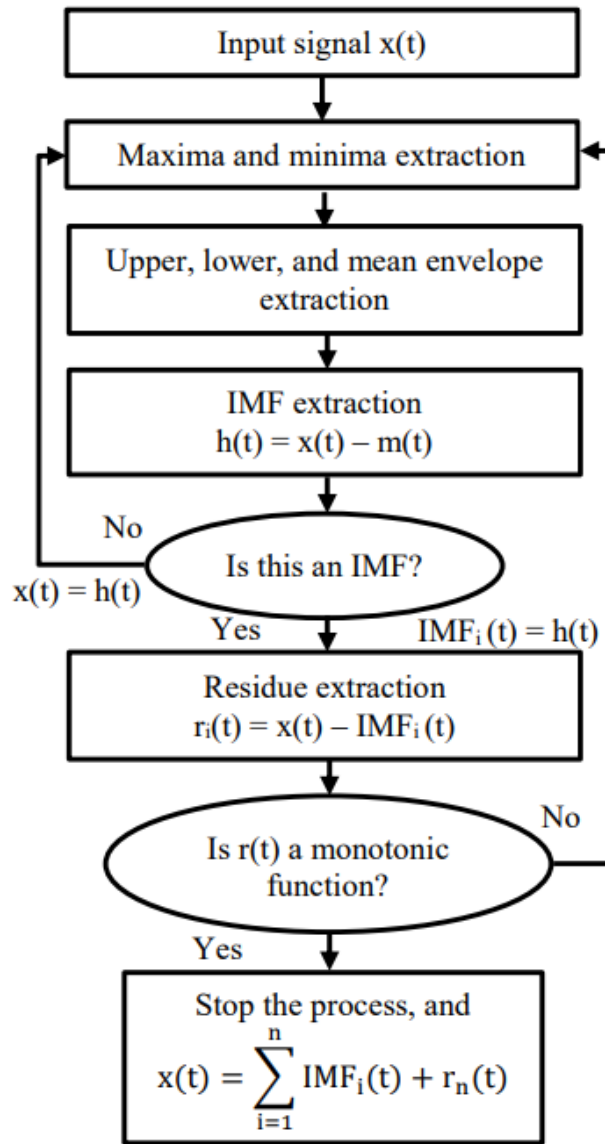


Figure 2.8 : The flowchart of EMD [37]

3. EXPERIMENTAL STUDY

3.1 Description of Test Bench

In this thesis, Bosch’s gasoline high-pressure pump endurance run test machine is used for measurements. This machine has been employed for product validation purposes, accurately simulating the working conditions of a pump. The test bench's mechanical system consists of several components: an electric motor (used for drive), a low-pressure fuel supply pump, couplings, a flywheel, a bearing support unit, a camshaft box, a high-pressure pump, and an encoder. Figure 3.1 and Figure 3.2 provide a schematic presentation and a front view of the test bench, respectively. Alongside the mechanical system, there is also a hydraulic part, which includes the fuel system, oil supply system, and heaters. Consequently, the test bench represents a complex system, encompassing real-world challenges such as measurement noise.

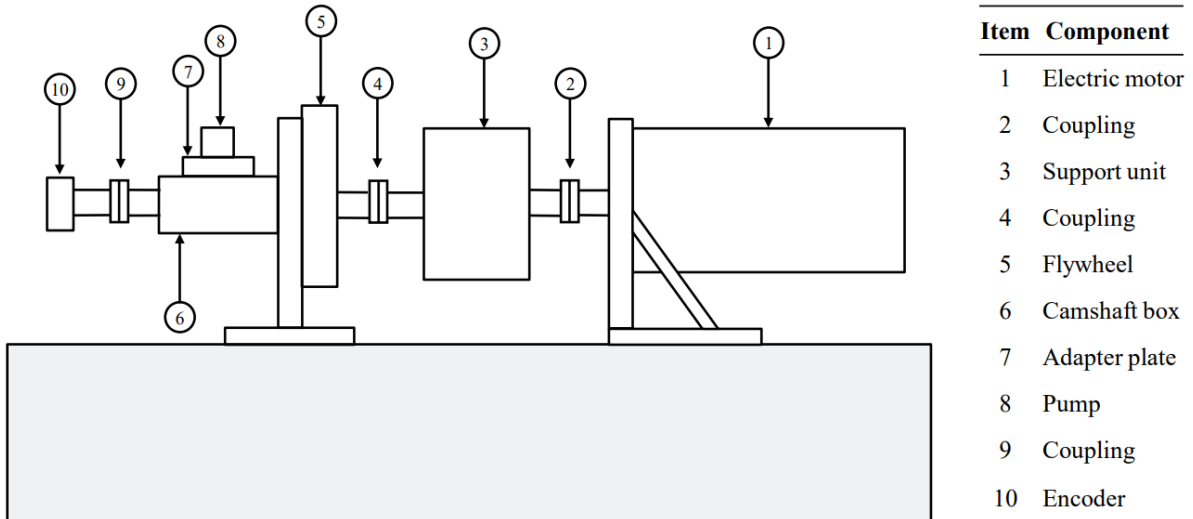


Figure 3.1 : Schematic presentation of the test bench

The high-pressure pump is driven by an electrical motor that provides the torque. An optical encoder, which measures the rotational speed, is located at the other end of the shaft, close to the faulty bearing. The system is loaded through the operation of the high-pressure pump, and there is no additional external load source in the system.

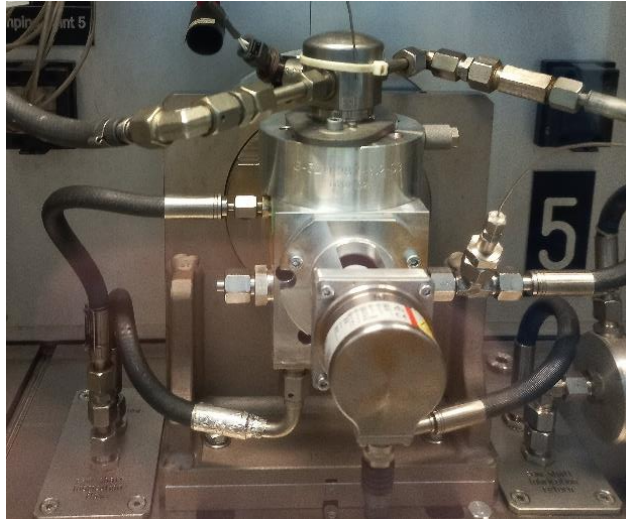


Figure 3.2 : Front view of the test bench

For bearing fault detection purposes, a camshaft box cylindrical roller bearing is used. Additionally, there are also bearings in the support unit and electrical motor. However, these are not within the scope of this investigation. The main bearing characteristic frequencies are given in Table 3.1.

Table 3.1 : Main characteristic frequencies.

The rotating order	1
The inner ring fault characteristic order	7.75
The rotating frequency (Hz)	7.5
The inner ring fault characteristic frequency (Hz) (BPFI)	58.13

For the ease of processing the defective bearing, a NJ205 type bearing featuring a detachable inner ring was selected as the test bearing. The Ball Pass Frequency Inner race (BPFI) characteristic frequency of this bearing is provided in Table 3.1 at 450 rpm. Grooves, each measuring 10 mm in length, 0.25 mm in depth, and having widths of 1 and 2 mm, were created on the inner ring through a milling process. The configuration of the fault is depicted in Figure 3.3.

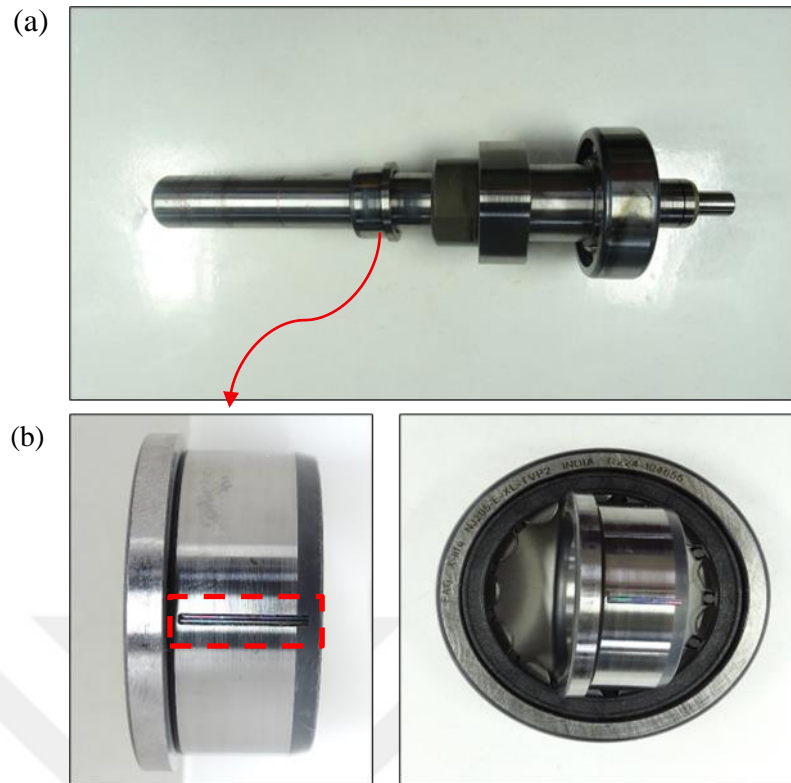


Figure 3.3 : (a) Camshaft, (b) Artificial fault, created on bearing inner ring

For simplicity, the length of the faults is set large enough to cover the roller ring contact zone. It is important to note that, in reality, spalls do not typically have this length, especially in the initial stages [47].

3.2 Measurement Campaign

In this experiment, three distinct measurements were conducted. M1 represents the baseline measurement with the bearing in a fault-free state, while M2 and M3 correspond to faulty measurements, characterized by fault widths of 1 mm and 2 mm, respectively. Alongside these, measurement parameters were specifically focused on sweeping the camshaft speed under a maximum pump outlet pressure of 35MPa, ranging from 300 rpm to 3625 rpm with 50 rpm increments. An example of the measurements can be seen in Figure 3.4.

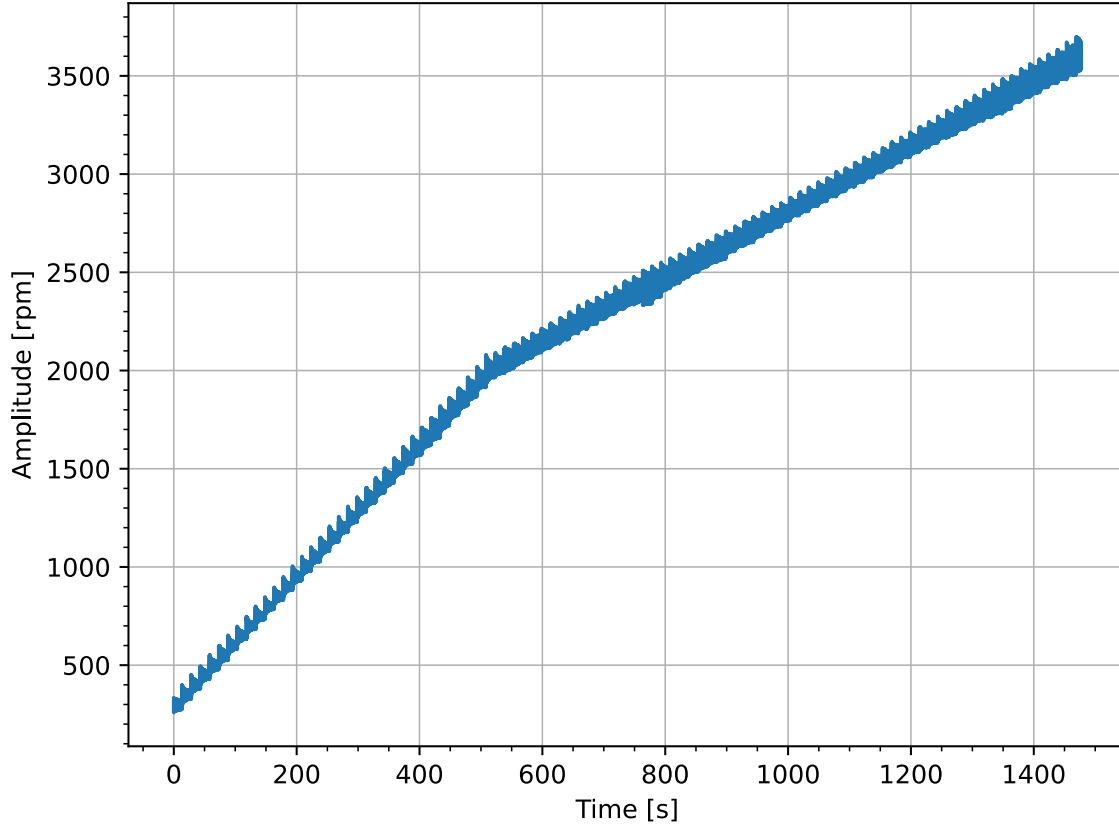


Figure 3.4 : Example measurement

The encoder, which has a resolution of 1000 PPR, transmitted its signal to a computer via a data acquisition system. This signal was sampled at a frequency of 50 kHz. To ensure the encoder's resolution and the accuracy of the rotational speed measurement, the minimum sampling frequency of the encoder's square signal was set to relatively high value. The appropriate sampling frequency is calculated using the following equation [7]:

$$F_s = 4x[Rf_{shaft} + (O_{max}f_{shaft} + R\Delta f)] \quad (3.1)$$

where R is the encoder resolution, f_{shaft} notates shaft rotating frequency, O_{max} is the highest order of interest, Δf is the IAS estimated speed variation.

4. SIGNAL PROCESSING AND RESULTS

In the present chapter, some of the main signal processing and bearing fault detection techniques have been investigated. Additionally, a synthesis of these techniques has been pursued to formulate effective methods. In the initial sub-chapter, well-established techniques, namely spectral kurtosis, and an envelope analysis-based methodology, were thoroughly examined. The subsequent sub-chapter introduces the development of a hybrid method integrating singular value decomposition and empirical mode decomposition (EMD) for the purpose of bearing fault detection.

4.1 Spectral Kurtosis and Envelope Analysis Based Method

As stated earlier, local faults in roller bearings produce a series of impacts which excite the resonance of the system. These periodic impacts are modulated by the resonance frequency of the system. As a result of the modulation process, a more complex signal arises, and it should be demodulated to obtain diagnostic information. Envelope analysis is one of the strong and relatively well-established techniques for bearing diagnostics [38]. It enables the demodulation of the signal by filtering out the fault (envelope) signal from the carrier (resonant) signal. However, one of the debates on envelope analysis is how to select the most plausible range for demodulation. This issue has been substantially addressed through the utilization of spectral kurtosis and kurtogram to identify the most impulsive range [38].

In this section, SK is used to detect the most impulsive band of the signal. By band-pass filtering this band, while removing signals elsewhere, the fault signal quality may be improved, and the kurtosis: a typical measure of the signal's peakedness [39], is increased. The signal is then filtered around the obtained frequency band. As a last step, envelope analysis is implemented on the band-pass filtered signal. The flowchart of the applied method is presented in Fig. 4.1.

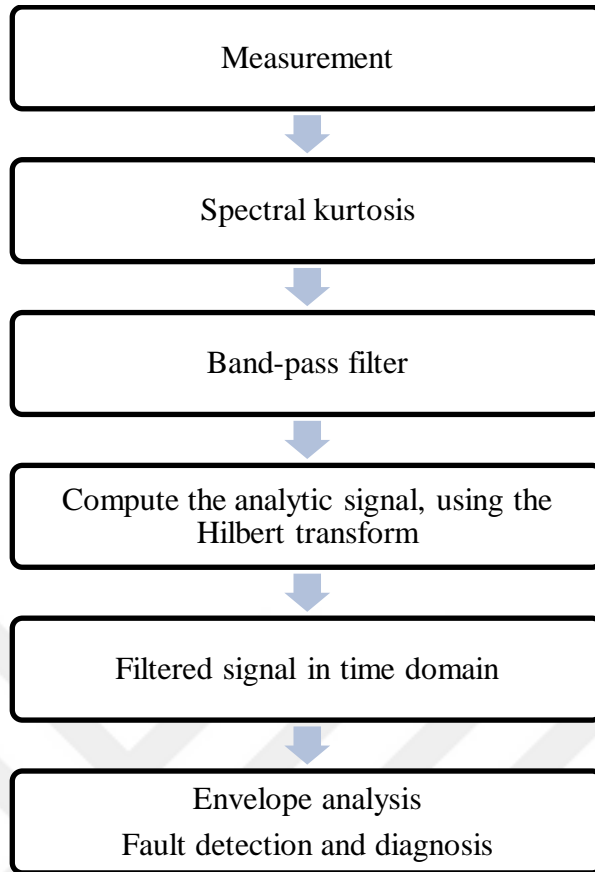


Figure 4.1 : Flowchart of applied method in section 4.1

In traditional vibration signals captured using accelerometers, the frequency components indicative of a bearing fault are typically low and frequently obscured within the overall structural response of the bearing. When measuring IAS variations from an encoder, the issue is that deterministic components, like shaft and gear frequencies, are prominent. Hence, fault frequencies have low energy in the signal [31]. In our case, there is no gear; however, shaft rotating frequency and high-pressure pump piston movement frequencies are strictly dominant in the spectrum. The piston movement frequency is equivalent to four times the shaft rotating frequency since it is driven by a four-lobe camshaft.

For the signal analysis, M1, M2 and M3 measurements which were acquired at 450 rpm are used. SK results of the three measurements are presented in Figure 4.2. Two bands are significant in measurements. For the M1 fault-free measurement, optimal-band corresponds to a band pass filter with center frequency $f_c = 18766.3$ Hz and bandwidth $b_w = 12500$ Hz.

For the M2 and M3 faulty measurements fast kurtograms are very similar, two band: band with $f_c = 18766.3$ Hz, $b_w = 12500$ Hz and band with $b_w = 3922.5$ Hz, $b_w = 1562.5$ Hz are

dominant and have higher kurtosis value. Therefore, the signals are investigated at two different bands and results are presented separately.

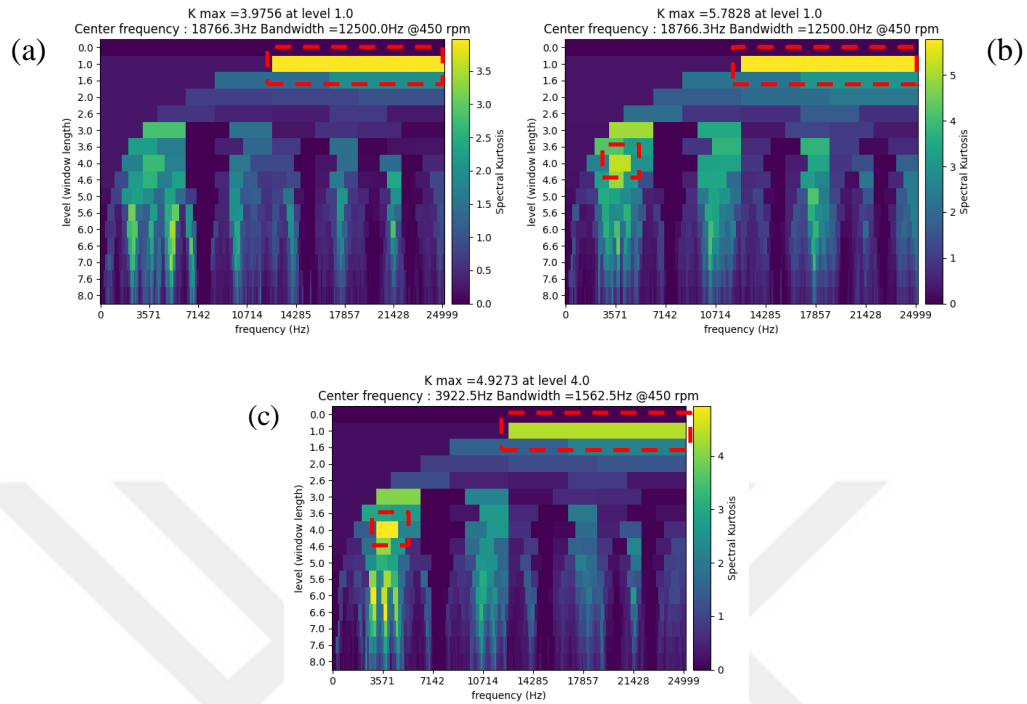


Figure 4.2 : Fast kurtogram: (a) M1 fault-free measurement; (b) M2 measurement with 1 mm fault width; (c) M3 measurement with 2 mm fault width.

In Figure 4.3, the envelope spectra of the M1 fault-free measurement are presented. There is no sign of BPF1 and harmonics at both bands. In contrast to the M1 measurement, BPF1 and harmonics are observed in the envelope spectra of the M2 and M3 measurements as can be seen in Figure 4.4. Even when the fault width is expanded from 1 mm to 2 mm in the M3 measurement, the second harmonics of the fault frequency become more visible.

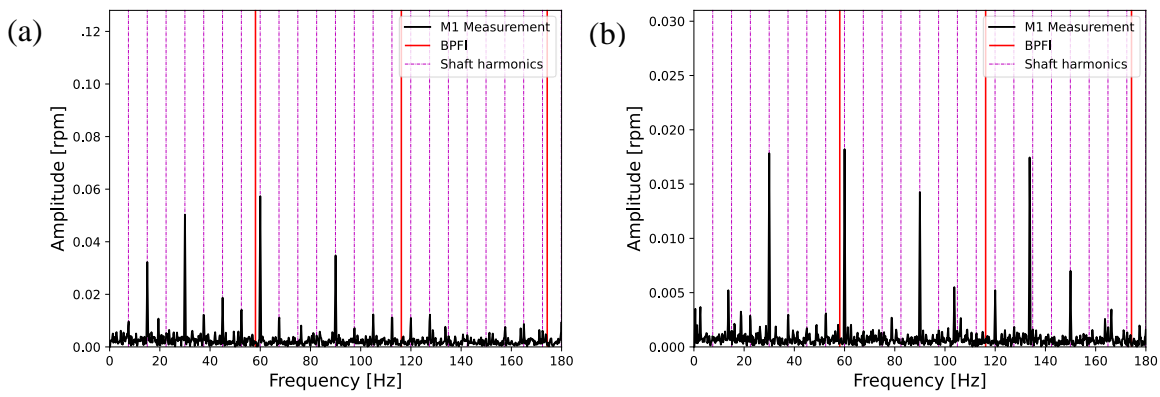


Figure 4.3 : Envelope spectrum of M1 fault-free measurement: (a) band pass filtered with $f_c = 3922.5$ Hz and $b_w = 1562.5$ Hz; (b) band pass filtered with $f_c = 18766.3$ Hz and $b_w = 12500$ Hz.

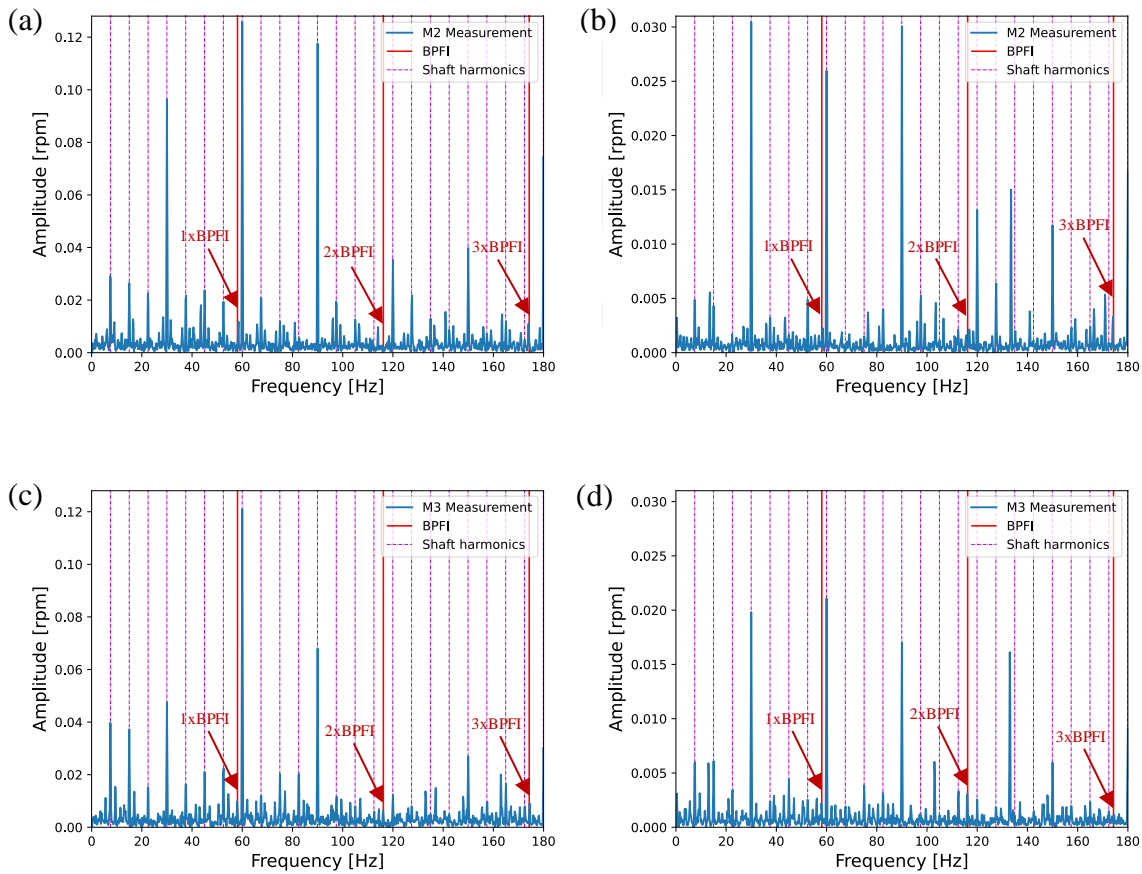


Figure 4.4 : Envelope spectrum of M2 and M3 faulty measurements: (a) M2 band pass filtered with $f_c = 3922.5$ Hz and $b_w = 1562.5$ Hz; (b) M2 band pass filtered with $f_c = 18766.3$ Hz and $b_w = 12500$ Hz; (c) M3 band pass filtered with $f_c = 3922.5$ Hz and $b_w = 1562.5$ Hz; (d) M3 band pass filtered with $f_c = 18766.3$ Hz and $b_w = 12500$ Hz

Another observation is that different speeds and frequency bands were investigated (not all are given here to avoid complexity). However, the shaft rotating frequency, piston movement frequencies, and their harmonics are always dominant in the signal. It has been concluded that most deterministic components should be removed from the signal since the bearing fault frequencies have low energy in the signal.

4.2 SVD and EMD Based Method

In this section, we introduce a signal de-noising and enhancement approach that employs a hybrid combination of SVD and Empirical Mode Decomposition. The efficacy of this method in detecting bearing fault is compared with raw signal and direct EMD applied signal's spectrums. For the signal analysis, M3 measurement which was acquired at 450 rpm is used. As outlined in section 3.2 measured signal contains 200000 data points spanning a duration of 4 seconds. Consistent with the concept of Instantaneous Angular Speed (IAS), shaft rotating speed instantaneously changes over time and fluctuates about average rotating speed. It can be easily understood from the time domain part of Figure 4.5.

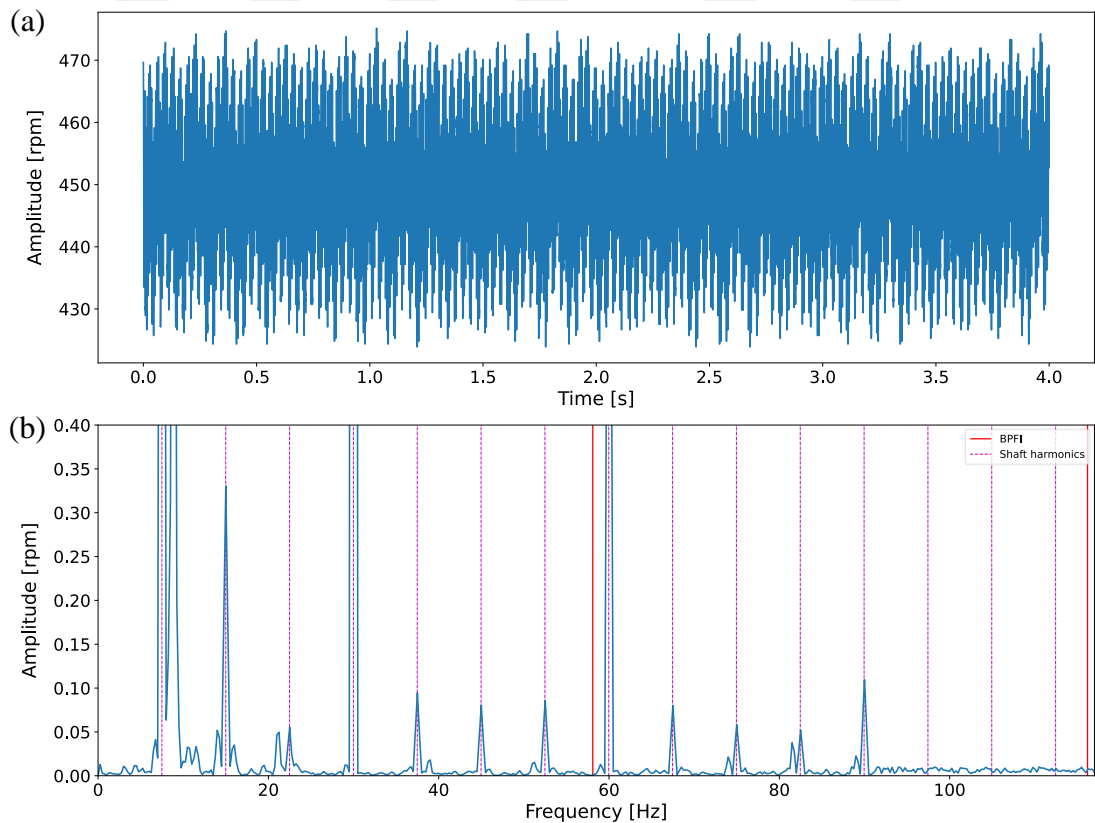


Figure 4.5 : (a) Captured IAS signal from a faulty bearing: M3 measurement, (b) corresponding amplitude spectrum.

The amplitude spectrums are plotted to encompass the first two harmonics of the bearing fault frequency. The second harmonic of the bearing fault frequency is approximately equal to 116 Hz. Therefore, spectrums are plotted up to 120 Hz. When the amplitude spectrum of the measurement was examined, it was not possible to detect bearing inner ring fault frequency.

In another investigation, EMD method is directly applied to the raw signal without any prior noise elimination. The first six Intrinsic Mode Functions (IMFs) and their corresponding amplitude spectrums are presented in Figures 4.6 and 4.7.

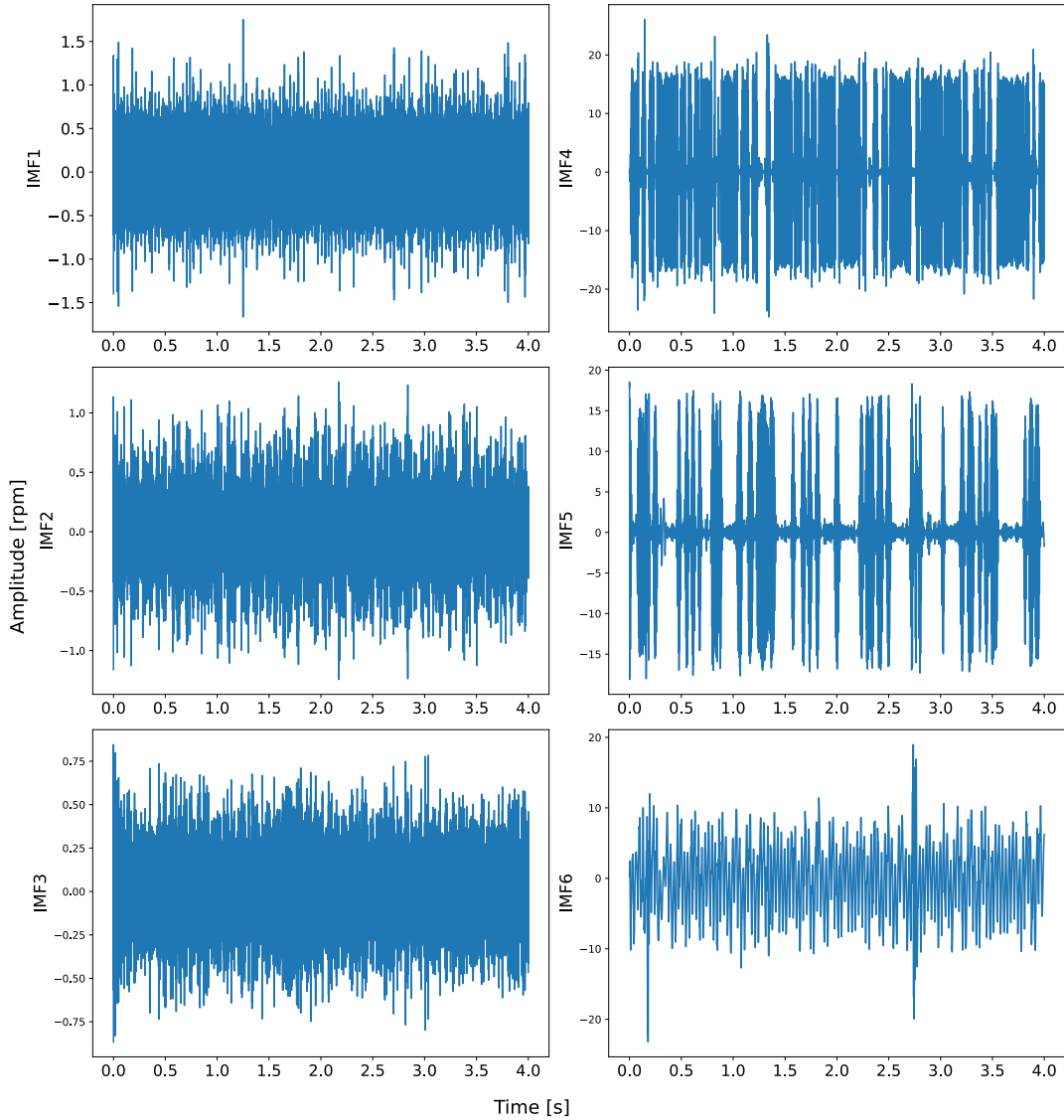


Figure 4.6 : The first six IMFs of the raw signal.

Each IMF of the signal is examined through the spectrum analysis. However, bearing inner ring fault frequency was not detectable in amplitude spectrums. Instead, the spectra were predominantly characterized by shaft harmonics and the high-pressure

pump piston movement frequency, which is equivalent to four times the shaft rotating frequency (30 Hz).

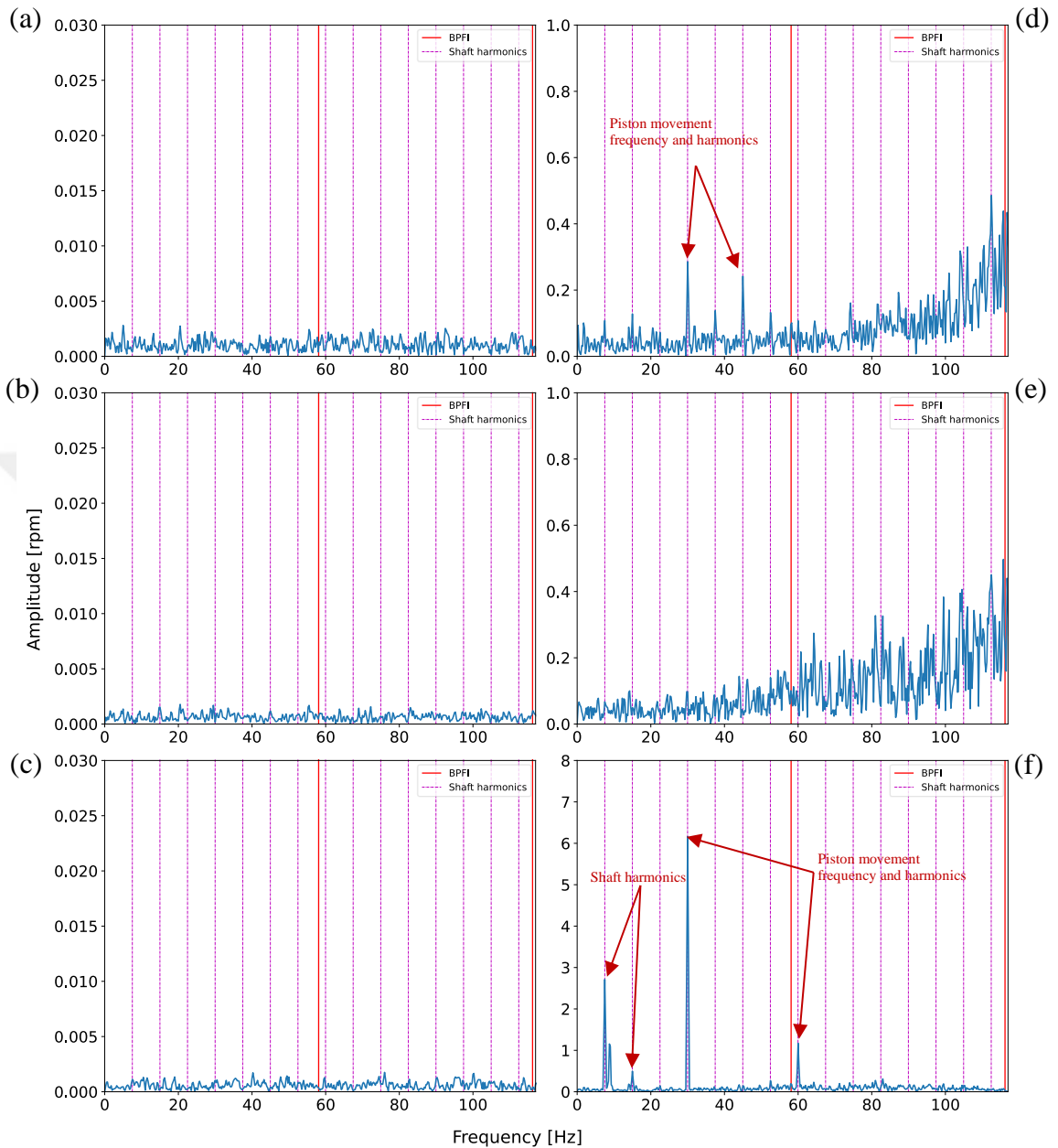


Figure 4.7 : Raw data EMD applied; amplitude spectrum of first six IMF: (a) IMF1, (b) IMF2, (c) IMF3, (d) IMF4, (e) IMF5, (f) IMF6

In proposed method, the SVD method is used for de-noising the signal in the time domain while the EMD method is employed to decompose the signal into different frequency bands. Then, signal is analysed to detect bearing fault using FFT in frequency domain. The flowchart of the proposed method is presented in Fig. 4.8.

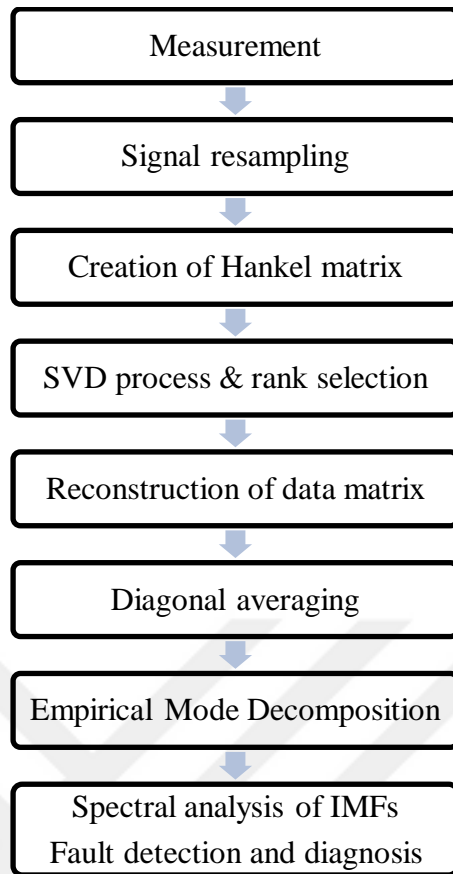


Figure 4.8 : Flowchart of proposed method in section 4.2

The proposed methodology is investigated using measured bearing instantaneous angular speed (IAS) signals. Despite instantaneous angular speed signal's insensitivity to the bearing transfer function, the measurement of rotational speed remains vulnerable to background noise [31]. Consequently, the SVD method is employed first to remove noise from the measured signal as much as possible. However, the SVD method is not directly applied to the measured raw signal since it was acquired at a very high sampling frequency and consists of huge number of data points. As the theoretical background of SVD is explained in section 2.6.1, this technique requires considerable computational time and performance based on the size of the input data matrix. Therefore, the raw data is resampled prior to SVD operation, but the frequency resolution is kept as before. The resampling frequency, on the other hand, is set to a certain value so as to guarantee that analysis spans the frequency range of interest for the purpose. Therefore, original signal is resampled to 70000 data points using the Fourier method, implemented via a built-in function in the Python SciPy library. This process is similar to interpolation, where the signal is reconstructed with fewer data points while maintaining the original signal's shape.

In the next step, the input signal in vector form is converted into a matrix form through Hankel matrix [48]. Later, input data matrix is decomposed using SVD method and singular values matrix is obtained. These singular values represent the strength or importance of different components in the signal. Larger singular values correspond to components that contribute more significantly to the overall structure of the signal. In the context of signal de-noising, identifying and retaining these larger singular values becomes crucial. They represent the dominant features or patterns in the signal, making them essential for preserving meaningful information while eliminating noise [22]. Therefore, during the de-noising process, a focus on larger singular values aids in effectively separating and preserving the significant components of the signal. One way to determine the first r singular values in equation 2.23, consequently the noise threshold is to plot the normalized singular values and to select the suitable rank when these normalized values near an asymptotic level [16, 49]. In total, 5000 singular values are calculated, but only 2000 of them are plotted. The first 2000 normalized singular values are plotted on a logarithmic scale, as shown in Figure 4.9.

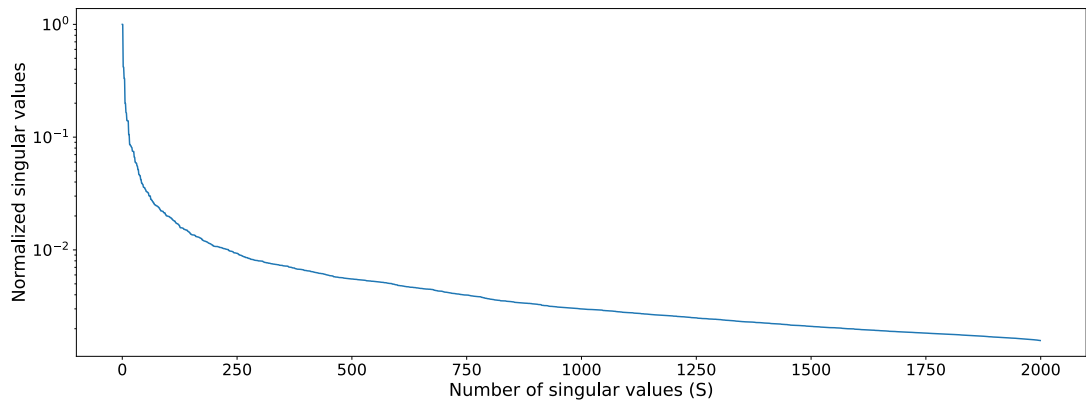


Figure 4.9 : Normalized singular values of Hankel matrix.

Upon analysing the plotted graph of normalized singular values, it was decided to investigate the impact of rank selection on signal noise elimination regarding different rank values: 50, 350, and 2000. Original and reconstructed signals are given in Figure 4.10.

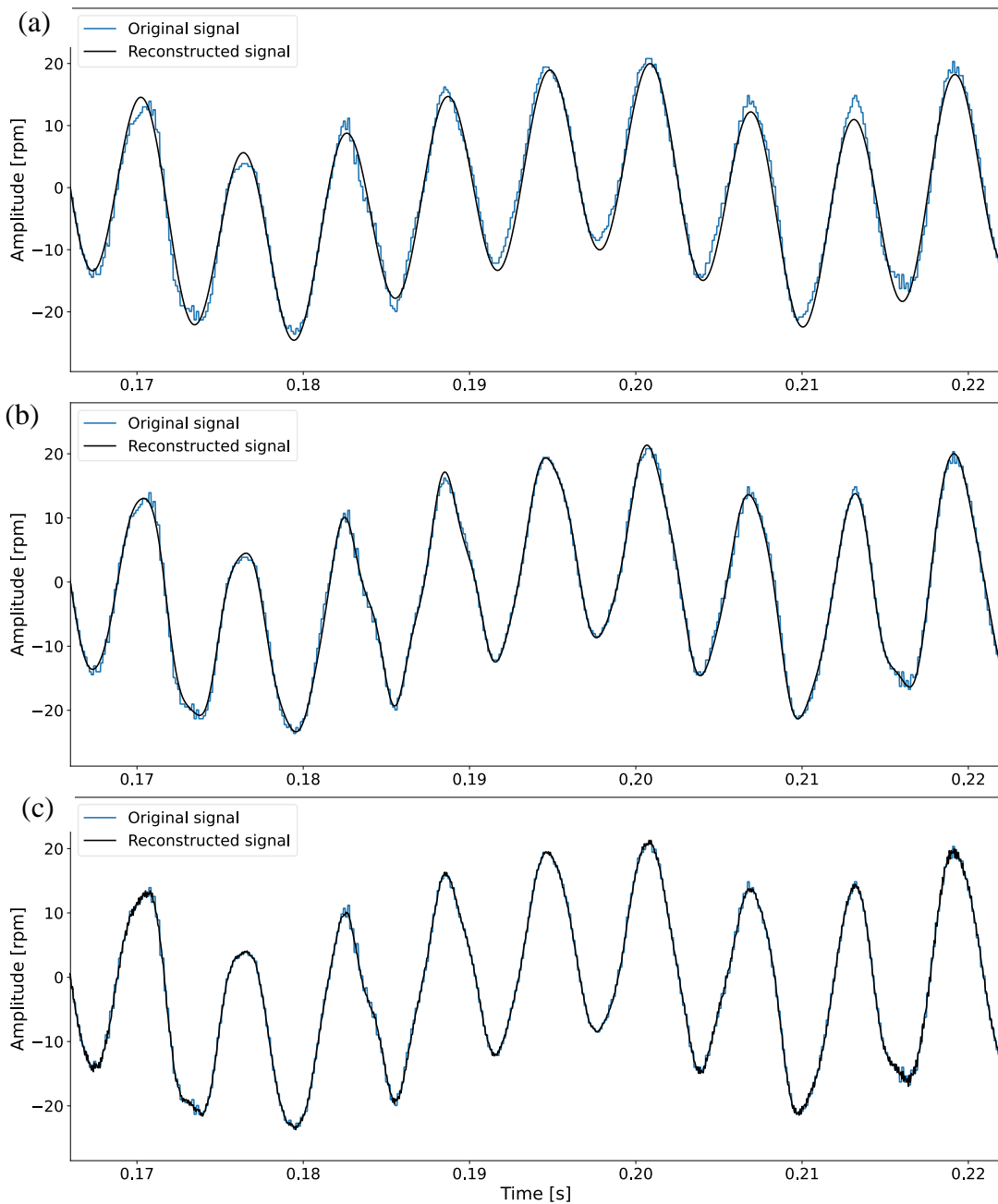


Figure 4.10 : Time waveform of original signal and reconstructed signal: (a) $r = 50$, (b) $r = 350$, (c) $r = 2000$

As illustrated in Figure 4.10, when a relatively low signal rank is chosen ($r = 50$), the reconstructed signal diverges from the original signal, resulting in a change in shape that may lead to information loss. Conversely, selecting a high rank value can lead to a significant reduction in signal noise elimination performance, with the increase of rank signal approaches to its original form as expected. Obviously, when the possible maximum rank is selected, the reconstructed signal becomes exactly the same as the original signal.

After the assessment of normalized singular values, effective rank value is chosen as 350 and data matrix is reconstructed based on the selected rank value. It is worth stating here that the reconstructed signal in vector form is derived through arithmetic averaging across the anti-diagonals of the reconstructed matrix. This technique, commonly referred to as diagonal averaging, details of the technique is explained in [22].

After the de-noising process, the de-noised signal is decomposed into intrinsic mode functions to distinguish different frequency bands. The first six IMFs are obtained and presented in Figure 4.11.

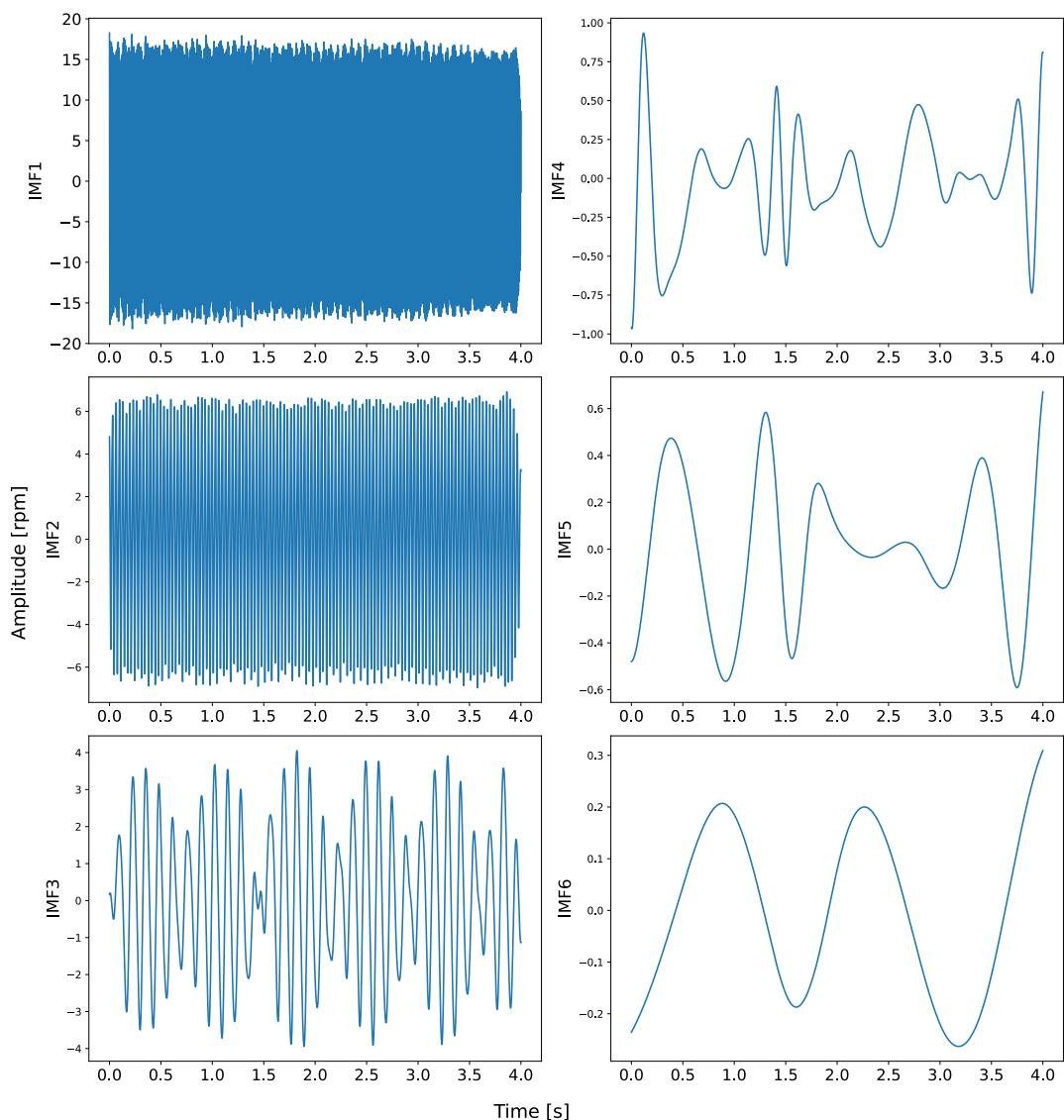


Figure 4.11 : The first 6 IMFs of the de-noised signal.

As can be seen in amplitude spectrums of the first six IMF in Figure 4.11, each IMF signal encapsulates a range of different frequency bands, spanning from high to low

frequencies. IMF1 includes the highest frequency component while the IMF6 represents the lower one in this set. It is suggested in the literature that by examining each of the IMFs, fault frequency of bearings may be identified [35].

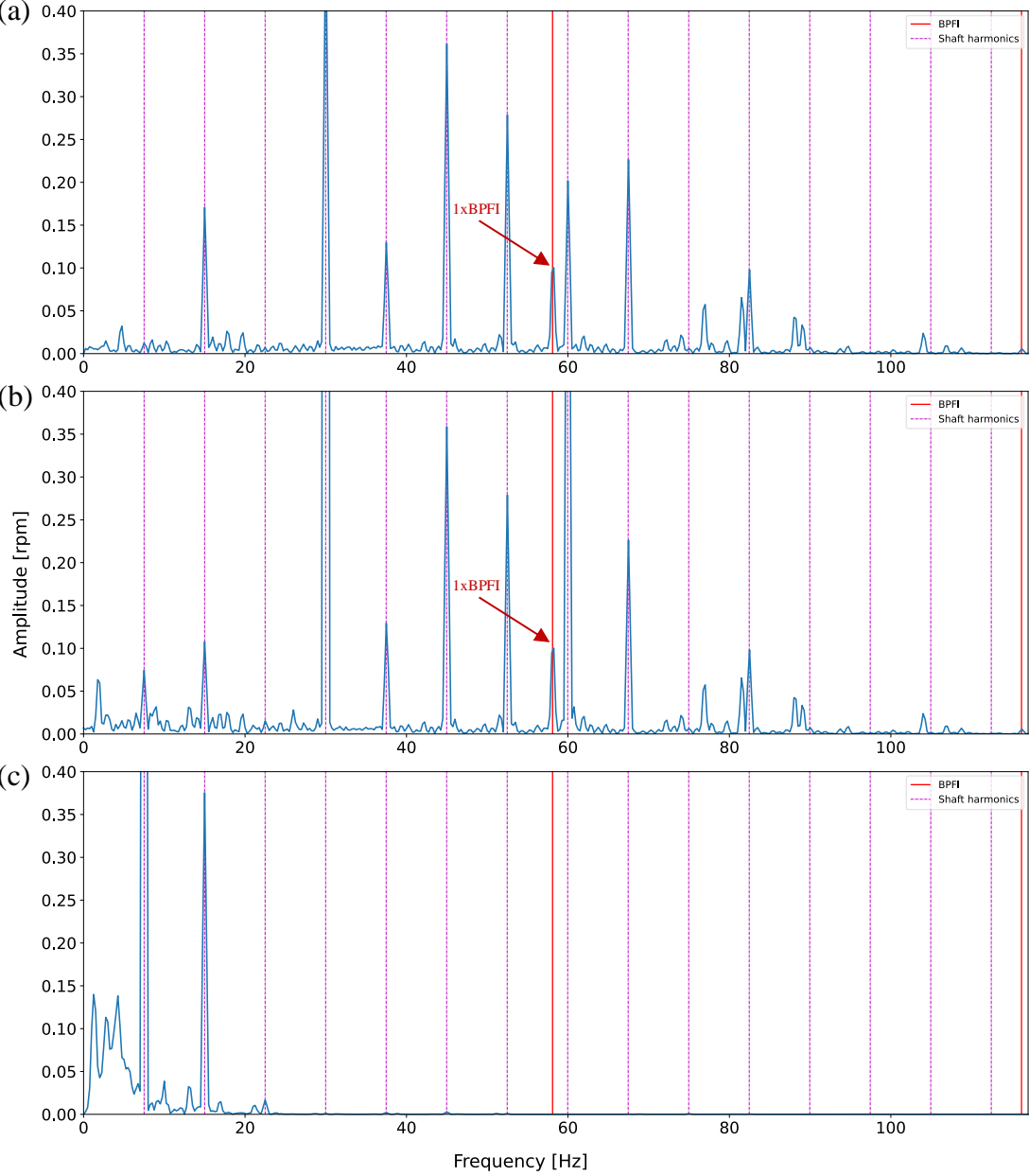


Figure 4.12 : Amplitude spectrums of first three IMF: (a) IMF1, (b) IMF2, (c) IMF3

When the presented spectrums in Figure 4.12 are examined, the bearing inner ring fault frequency (BPF1) is distinctly visible in the first two IMF’s amplitude spectrum. On the other hand, the third IMF’s amplitude spectrum is dominated by the rotational frequency of the shaft and this makes other components of the signal greater than about 20 Hz not notable. It is demonstrated that bearing inner ring fault frequency can be

successfully detected with proposed method under fairly strong background noise while direct EMD method shows weak performance.

4.3 Fault Detection Method Based on Removal of Deterministic Components

As highlighted earlier, in standard accelerometer-based vibration measurements, the frequency components indicative of a bearing fault carry low-energy and are typically integrated into the structural response of the bearing housing. However, when analyzing instantaneous angular speed variations captured by an encoder, the challenge shifts, it becomes critical to eliminate the most energetic components that do not pertain to the target frequencies. It is essential to eliminate frequencies associated with the shaft and gears. In our case, despite the absence of gears in the system, frequencies related to piston movements and shaft harmonics were notably prevalent in the signal. While various techniques are available such as Linear Prediction, Time Synchronous Averaging (TSA), etc. The removal of deterministic components in this context is achieved through the Fourier domain, by setting the corresponding Fourier coefficients in the signal to zero. This method bears resemblance to the practice of comb filtering.

In this method, windowing (Hanning window) is initially applied to the signal to reduce spectral leakage prior to the filtering operation. Following the windowing process, the signal's amplitude spectrum is analyzed to identify the frequency bands around the center frequencies that need filtering. The center frequencies and their adjacent Fourier coefficients are then set to zero. Once the signal has been filtered in the frequency domain, an Inverse Fourier Transform (IFFT) is performed on the signal to revert it to the time domain. Additionally, both before and after filtering, the RMS and kurtosis values of the signals are computed and recorded. For spectral analysis, a Fourier transform is conducted on the filtered signal. Since windowing was applied before the filtering, it is not reapplied before the FFT operation; as the edges of the time domain signal were already close to zero, there would not be a sharp transition in the FFT operation. The effects of windowing and the optimal placement of the window in this method were explored, with the best performance achieved following this sequence. The flowchart of the proposed method is clearly depicted in Fig. 4.13.

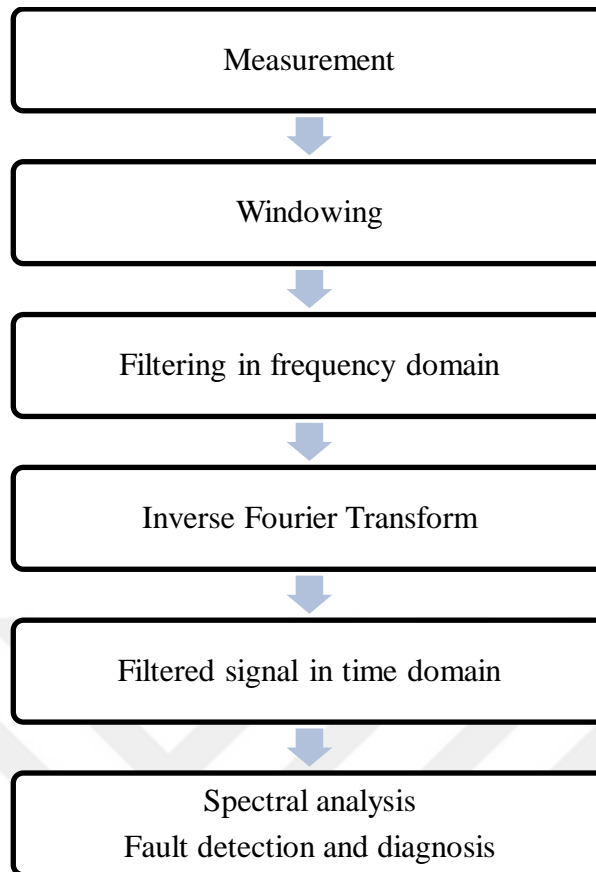


Figure 4.13 : Flowchart of proposed method in section 4.3

The M3 faulty measurement signal is utilized to test the proposed method, analyzed at various working speeds. To illustrate the condition before filtering, FFT is directly applied to the signal at 300 rpm, with similar outcomes observed at other speeds. A relatively lower rpm is chosen due to its lower noise content. As shown in Figure 4.14, without any signal cleaning or filtering, it is impossible to detect the bearing inner fault frequency since the energy of the bearing fault frequency is very low in the signal.

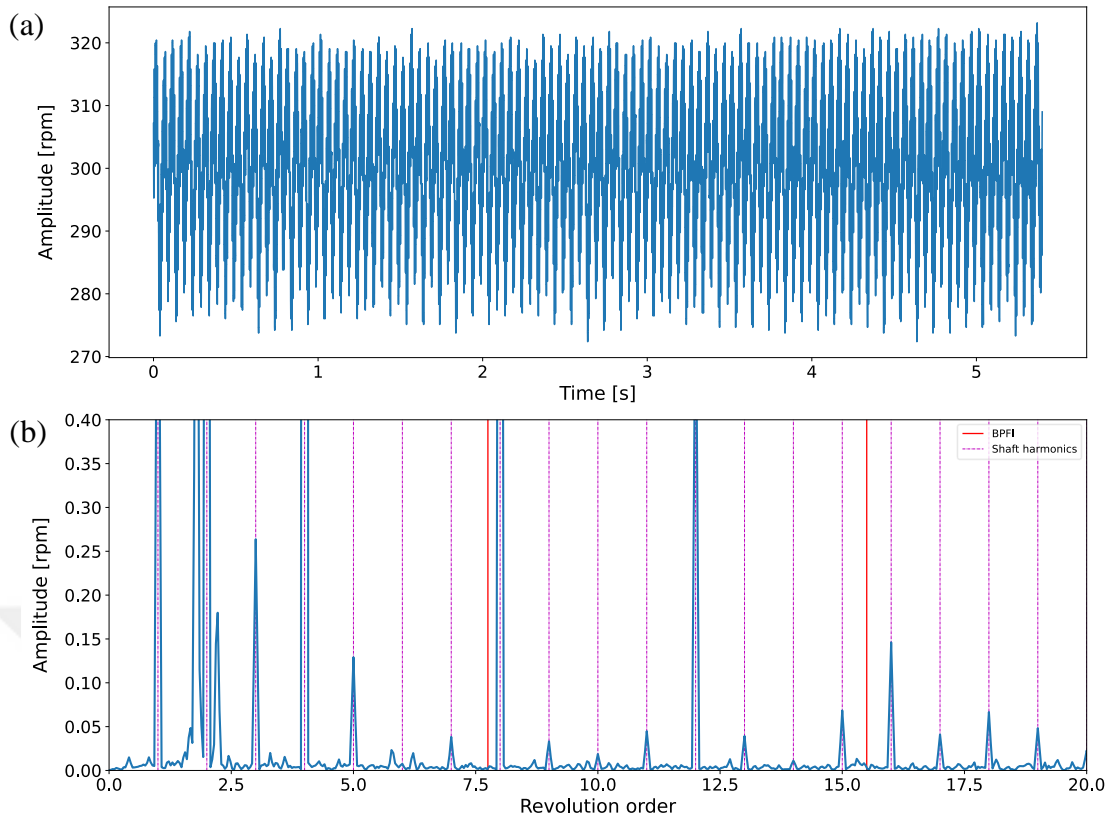


Figure 4.14 : (a) Captured IAS signal from a faulty bearing at 300 rpm: M3 measurement, (b) corresponding amplitude spectrum.

To demonstrate the method's effectiveness, signal spectra are analyzed at various speeds. The amplitude spectra and the envelope spectrum are presented in Figs. 4.15, 4.16, and 4.17 for different speeds.

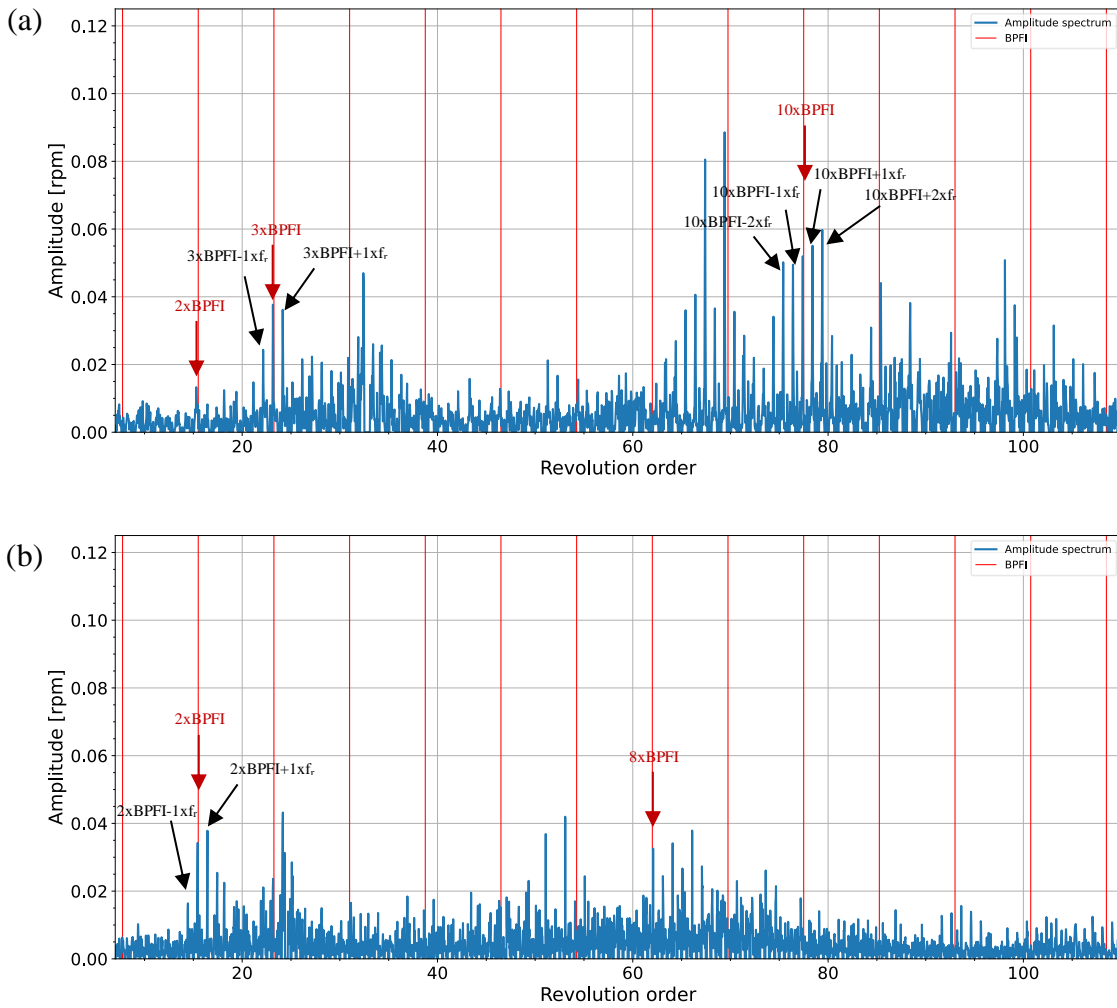


Figure 4.15 : Amplitude Spectra of filtered IAS signals at: (a) 300 rpm, (b) 400 rpm

When the spectra are analyzed, frequencies and harmonics associated with bearing inner ring fault is detected in both amplitude and envelope spectra. A review of the literature anticipated the presence of particularly high harmonics in incipient faults, a characteristic that is observed in this study as well. Additionally, when the fault is present on a rotating component, signal modulation occurs. In our case, the bearing inner ring rotates along with the mounted shaft. Consequently, the bearing inner ring fault frequency is modulated by the shaft rotation frequency. This modulation can be monitored as sidebands around the center frequency in the spectra. These can be observed in the relevant spectral plots as $1x\text{BPFI} \pm 1x\text{fr}$, $1x\text{BPFI} \pm 2x\text{fr}$, $2x\text{BPFI} \pm 1x\text{fr}$, $2x\text{BPFI} \pm 2x\text{fr}$, etc.

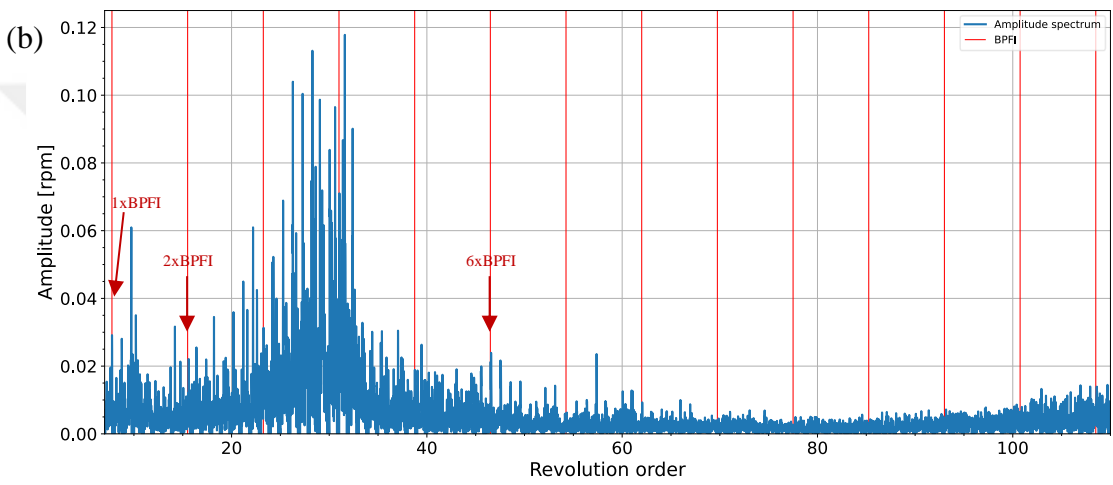
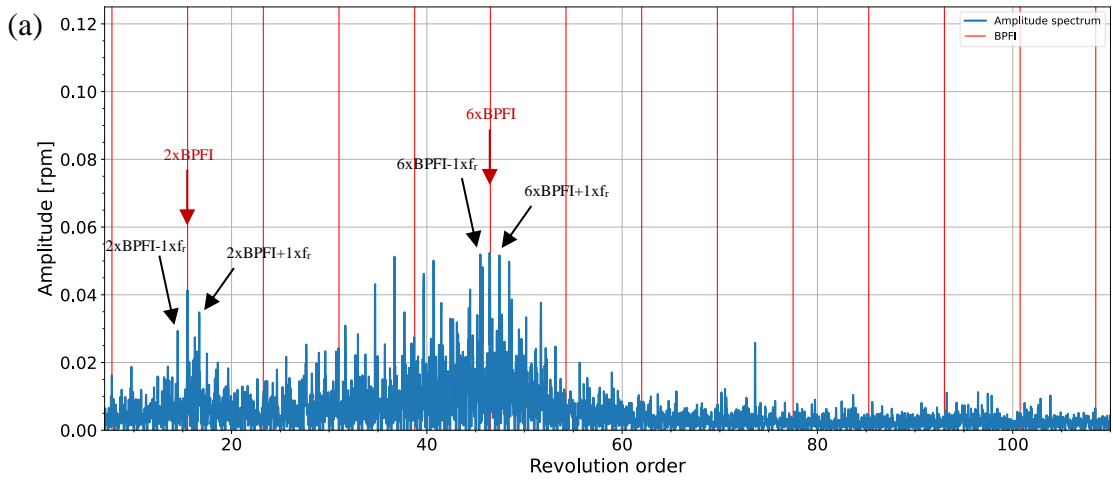


Figure 4.16 : Amplitude Spectra of filtered IAS signals at: (a) 600 rpm, (b) 1000 rpm

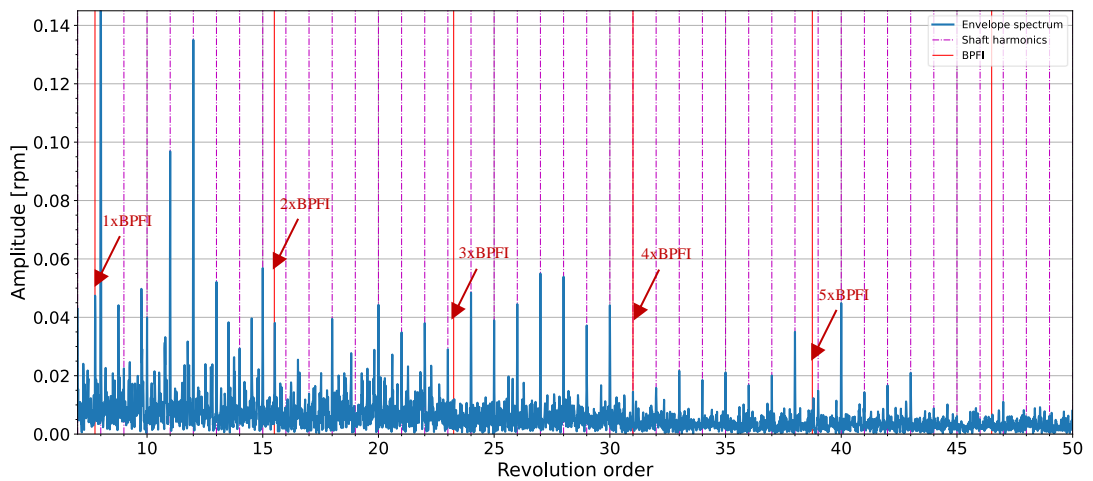


Figure 4.17 : Envelope spectrum of filtered IAS signal at 1000 rpm.

When investigating the effect of working speed, consistent results were obtained in amplitude spectra at different working speeds, where the bearing inner ring fault frequency could be detected. However, the results in the envelope spectra were not as consistent as those in the amplitude spectra at certain speeds. It was not possible to detect bearing inner ring fault frequency at whole speeds. Another observation is that the amount of noise in the signal increases with increasing speed, making it harder to distinguish the bearing inner ring fault frequency and its harmonics in the spectra. Therefore, it is observed that speeds lower than 1000 rpm yield better results in our application. For similar applications, lower speeds are recommended for improved fault detection performance. When comparing the kurtosis and RMS values of the filtered and original signals, it is noted that after filtering, both the kurtosis and RMS values of the signals are increased. A similar behavior is observed with the amount of noise in the signal; both RMS and kurtosis values are increased with the increase in working speed.

5. CONCLUSIONS AND SUGGESTIONS

5.1 Conclusions

This thesis aims to assess methodologies for fault detection of roller bearings based on rotary encoder signals. The most common and well-established signal processing techniques used in traditional vibration-based fault detection applications are examined, and their implementations in encoder-based fault diagnosis are investigated. Particular attention is devoted to the enhancement and de-noising aspects of the measured signals to increase the fault detection performances of the method studied.

After the introduction of the problem and a review of the existing literature, the second chapter focuses on encoder specific parts, wherein working principle and measurement, employed signal processing methods are introduced.

In the third chapter, the experimental setup, and the details of the measurement campaign are described.

In the experimental part of the study, an already existing test bench for the endurance validation of high-pressure pumps is used. It enabled to carry out work on real-world measurements which also contain a significant amount of background noise.

Chapter 4 deals with signal processing of the measured raw data in order to get hidden information which can be utilised for bearing fault detection. Three main methodologies are introduced.

In the first methodology, spectral kurtosis (SK) and envelope analysis are used to detect bearing inner ring faults. For this purpose, fault-free as well as small, and medium fault sizes are examined. The effects of carrying out the analysis within different frequency bands on the performance of this method is also investigated. It is shown that the bearing inner ring fault frequency is detectable in the envelope spectra of the faulty bearings while there is no visible peak in fault-free measurement spectra. Moreover, it is found that when the fault size is increased, the second harmonic of the bearing inner ring fault frequency also becomes visible in the envelope spectrum.

In the second part of this section, signal de-noising was the primary focus of the investigation. Singular Value Decomposition (SVD) and Empirical Mode Decomposition (EMD) based bearing fault detection methodology is proposed. First of all, the spectrum of the unprocessed signal and EMD applied signals are examined to detect the bearing inner ring fault frequency. However, no indication of bearing fault frequency was detectable in the spectra. Then, the SVD method is employed as a pre-signal processing step for de-noising the raw signal. The details of the SVD method, including data matrix creation and effective rank selection, are also handled. After the signal de-noising process, the EMD method is utilised to decompose the signal into different frequency bands and intrinsic mode functions (IMFs) of the signal are obtained. Detailed investigation of IMFs reveals that the bearing inner ring fault frequency, hence the fault, can be confidently detected in the first two IMF spectra of the signal. Consequently, it is shown that the proposed methodology is capable of accurately identifying the bearing inner ring fault frequency even in the presence of fairly substantial background noise. However, only spectrum analysis and the direct application of Empirical Mode Decomposition (EMD) have shown limited efficacy under the same conditions.

In the third method, the most deterministic components are removed from the signal to highlight the bearing fault frequency. Kurtosis values are calculated for both the filtered and the original signals, with an observation that kurtosis values increase following the filtering operation. Post-filtering, both amplitude and envelope spectra are meticulously analyzed at various working speeds. In both spectra, the bearing inner ring fault frequency and its harmonics are successfully identified. However, the amplitude spectra display more consistent results across different working speeds. Thus, a hybrid methodology incorporating both amplitude and envelope spectra is recommended for generating fault indicators. Furthermore, upon examining the spectra, sidebands around the center frequencies become noticeable due to the modulation of the bearing fault frequency with the shaft rotating frequency, a phenomenon anticipated when the bearing fault is on the rotating components, as per the literature. It is also noted that with an increase in rotating speeds, the noise content of the signal escalates in our scenario. This increase is also reflected in the kurtosis values, making it easier to identify bearing fault frequencies at relatively lower rpms. In our case, speeds lower than 1000 rpms yield superior signal fault detection

performance. Therefore, fault detection at lower rpms is recommended for similar systems.

Consequently, it is concluded that encoder signal-based fault detection methods can be powerful alternatives in the field of condition monitoring of bearings. Moreover, it is found that the bearing fault detection capability of the methods can be significantly improved by the use of signal de-noising.



5.2 Suggestions for Future Works

When measuring instantaneous angular speed (IAS) variations from an encoder, a significant challenge arises due to deterministic components related to the kinematic chain, such as shaft and gear frequencies, which are prominent in the signal. Consequently, vibrations at fault frequencies exhibit low level of energy in the signal. In order to increase the relative contributions of the vibrations at fault-related frequencies, future research could focus on refining the techniques for the subtraction or cleansing of signals from various kinematic chain-related components.

Moreover, advanced investigations may be conducted about the proposed SVD-EMD based noise reduction and bearing fault detection method in this thesis. For the SVD part, researchers may develop appropriate methods for automatic selection of the effective rank, particularly tailored for torsional vibration signals. Even a minor improvement in rank selection procedure could significantly enhance the signal denoising performance and speed up the fault detection procedure.

Another potential area for improvement is the signal decomposition aspect of the method. While this study employs the most traditional and accepted version of the EMD method, various other EMD versions exist in the literature. These could be assessed, and the IAS signal-based fault detection method can be improved.

In the experimental validation part of this thesis, our research concentrated on a single fault in one bearing, despite the availability of other bearings in the system. Most industrial machines, as in our system, consist of various components and several bearings. Future studies can explore scenarios with multiple faults in a single bearing or multiple bearings.

Additionally, investigating the encoder fault detection capability in systems with multiple components, both in single and multiple drive trains, presents another challenging research direction.

REFERENCES

- [1] **Mohanty, A. R.** (2014). *Machinery condition monitoring: Principles and practices*. CRC Press.
- [2] **Randall, R. B.** (2021). *Vibration-based condition monitoring: industrial, automotive and aerospace applications*, Second ed., John Wiley & Sons, Illinois.
- [3] **Xu, X., Zhao, M., & Lin, J.** (2017). Detecting weak position fluctuations from encoder signal using singular spectrum analysis. *ISA transactions*, 71, 440-447.
- [4] **Li, Y., Gu, F., Harris, G., Ball, A., Bennett, N., & Travis, K.** (2005). The measurement of instantaneous angular speed. *Mechanical Systems and Signal Processing*, 19(4), 786-805.
- [5] **André, H., Bourdon, A., and Rémond, D.** (2011). On the use of the instantaneous angular speed measurement in non stationary mechanism monitoring. In *International Design Engineering Technical Conferences and Computers and Information in Engineering Conference* (Vol. 54785, pp. 15-24).
- [6] **Zhou, F. C., Tang, G. J., & He, Y. L.** (2016). An Effective gear fault diagnosis method based on singular value decomposition and frequency slice wavelet transform. *International Journal of Rotating Machinery*, 2016.
- [7] **Gu, F., Yesilyurt, I., Li, Y., Harris, G., & Ball, A.** (2006). An investigation of the effects of measurement noise in the use of instantaneous angular speed for machine diagnosis. *Mechanical Systems and Signal Processing*, 20(6), 1444-1460.
- [8] **Renaudin, L., Bonnardot, F., Musy, O., Doray, J. B., & Rémond, D.** (2010). Natural roller bearing fault detection by angular measurement of true instantaneous angular speed. *Mechanical Systems and Signal Processing*, 24(7), 1998-2011.

- [9] Zhou, Y., Tao, T., Mei, X., Jiang, G., & Sun, N. (2011). Feed-axis gearbox condition monitoring using built-in position sensors and EEMD method. *Robotics and Computer-Integrated Manufacturing*, 27(4), 785-793.
- [10] Li, Z., Yan, X., Yuan, C., & Peng, Z. (2012). Intelligent fault diagnosis method for marine diesel engines using instantaneous angular speed. *Journal of Mechanical Science and Technology*, 26, 2413-2423.
- [11] Spagnol, M., & Bregant, L. (2014). Instantaneous angular speed: encoder-counter estimation compared with vibration data. In *Advances in Condition Monitoring of Machinery in Non-Stationary Operations: Proceedings of the third International Conference on Condition Monitoring of Machinery in Non-Stationary Operations CMMNO 2013* (pp. 347-354). Springer Berlin Heidelberg.
- [12] Roy, S. K., Mohanty, A. R., & Kumar, C. S. (2016). Envelope analysis of instantaneous angular speed for fault detection in multistage gearbox. *Journal of Vibration Engineering & Technologies*, 4, 447-454.
- [13] Li, B., & Zhang, X. (2017). A new strategy of instantaneous angular speed extraction and its application to multistage gearbox fault diagnosis. *Journal of Sound and Vibration*, 396, 340-355.
- [14] Miao, Y., Zhao, M., Liang, K., & Lin, J. (2020). Application of an improved MCKDA for fault detection of wind turbine gear based on encoder signal. *Renewable Energy*, 151, 192-203.
- [15] Bourdon, A., Chesné, S., André, H., & Rémond, D. (2019). Reconstruction of angular speed variations in the angular domain to diagnose and quantify taper roller bearing outer race fault. *Mechanical Systems and Signal Processing*, 120, 1-15.
- [16] Sanliturk, K. Y., & Cakar, O. (2005). Noise elimination from measured frequency response functions. *Mechanical Systems and Signal Processing*, 19(3), 615-631.
- [17] Wang, Y. S., He, H., & Chen, X. W. (2009, June). Comparison and application of signal denoising techniques based on time-frequency algorithms. In *2009 IEEE Intelligent Vehicles Symposium* (pp. 129-133). IEEE.

- [18] **Zhao, X., & Ye, B.** (2009). Similarity of signal processing effect between Hankel matrix-based SVD and wavelet transform and its mechanism analysis. *Mechanical Systems and Signal Processing*, 23(4), 1062-1075.
- [19] **Abouel-Seoud, S. A., & Lemosry, M.** (2012). Enhancement of signal denoising and fault detection in wind turbine planetary gearbox using wavelet transform. *International Journal of Science and Advanced Technology*, 2(5), 120-131.
- [20] **Roy, S. K., Mohanty, A. R., & Kumar, C. S.** (2016). Fault detection in a multistage gearbox by time synchronous averaging of the instantaneous angular speed. *Journal of vibration and control*, 22(2), 468-480.
- [21] **Zhao, M., & Lin, J.** (2017). Health assessment of rotating machinery using a rotary encoder. *IEEE Transactions on Industrial Electronics*, 65(3), 2548-2556.
- [22] **Golafshan, R., & Sanliturk, K. Y.** (2016). SVD and Hankel matrix based denoising approach for ball bearing fault detection and its assessment using artificial faults. *Mechanical Systems and Signal Processing*, 70, 36-50.
- [23] **Zhao, M., & Jia, X.** (2017). A novel strategy for signal denoising using reweighted SVD and its applications to weak fault feature enhancement of rotating machinery. *Mechanical Systems and Signal Processing*, 94, 129-147.
- [24] **Zhang, Q., Zhao, W., & Xiao, S. G.** (2017, April). Fault diagnosis of gear based on singular value decomposition and RBF neural network. In *2nd International Conference on Frontiers of Sensors Technologies (ICFST)* (pp. 470-474). IEEE.
- [25] **Li, B., Zhang, X., & Wu, J.** (2017). New procedure for gear fault detection and diagnosis using instantaneous angular speed. *Mechanical Systems and Signal Processing*, 85, 415-428.
- [26] **Yin, X., Xu, Y., Sheng, X., & Shen, Y.** (2019). Signal denoising method using AIC-SVD and its application to micro-vibration in reaction wheels. *Sensors*, 19(22), 5032.
- [27] **Miao, F., Zhao, R., & Wang, X.** (2020). A new method of denoising of vibration signal and its application. *Shock and Vibration*, 2020, 1-8.

- [28] Miao, F., & Zhao, R. (2022). A new method of vibration signal denoising based on improved wavelet. *Journal of Low Frequency Noise, Vibration and Active Control*, 41(2), 637-645.
- [29] Ni, Z., Wang, X., Hong, Y., & Tang, G. (2022). Bearing inner race fault detection and size estimation using the variable reluctance sensor. *Journal of Sound and Vibration*, 530, 116968.
- [30] Sawalhi, N., & Randall, R. B. (2008). Simulating gear and bearing interactions in the presence of faults: Part I. The combined gear bearing dynamic model and the simulation of localised bearing faults. *Mechanical Systems and Signal Processing*, 22(8), 1924-1951.
- [31] Bertoni, R., & André, H. (2023). Proposition of a bearing diagnosis method applied to IAS and vibration signals: The BEARING Frequency Estimation Method. *Mechanical Systems and Signal Processing*, 187, 109891.
- [32] Gomez, J. L., Bahmani, A., Andre, H., Remond, D., & Bourdon, A. (2014). Non-stationary statistical fault indicators estimation applied on IAS machine surveillance. In *Proceedings of the Biennial ISMA Conference on Noise and Vibration Engineering, ISMA 2014, Leuven (Belgium), 15–17 Sept 2014*.
- [33] **The incremental encoder – operation principals & fundamental signal evaluation possibilities (part 1)**. Access: 12 December 2023, <https://www.imc-tm.com/download-center/white-papers/the-incremental-encoder-part-1/page>
- [34] Kim, S., An, D., & Choi, J. H. (2020). Diagnostics 101: A tutorial for fault diagnostics of rolling element bearing using envelope analysis in MATLAB. *Applied Sciences*, 10(20), 7302.
- [35] Sim, J., Min, J., Kim, D., Cho, S. H., Kim, S., & Choi, J. H. (2022). A python based tutorial on prognostics and health management using vibration signal: signal processing, feature extraction and feature selection. *Journal of Mechanical Science and Technology*, 36(8), 4083-4097.
- [36] Courrech, J., & Gaudet, M. (1998). Envelope analysis-the key to rolling-element bearing diagnosis. *Brüel & Kjaer Application Notes*.
- [37] Golafshan, R. (2015). *Vibration-based fault detection for ball bearings*. (Master thesis). Istanbul Technical University, Graduate School of Science Engineering and Technology, Istanbul.

- [38] **Randall, R. B., & Antoni, J.** (2011). Rolling element bearing diagnostics—A tutorial. *Mechanical Systems and Signal Processing*, 25(2), 485-520.
- [39] **Wang, Y., Xiang, J., Markert, R., & Liang, M.** (2016). Spectral kurtosis for fault detection, diagnosis and prognostics of rotating machines: A review with applications. *Mechanical Systems and Signal Processing*, 66, 679-698.
- [40] **Kurtosis.** Access: 12 December 2023, <https://community.sw.siemens.com/s/article/kurtosis>
- [41] **Antoni, J., & Randall, R. B.** (2006). The spectral kurtosis: application to the vibratory surveillance and diagnostics of rotating machines. *Mechanical Systems and Signal Processing*, 20(2), 308-331.
- [42] **Sawalhi, N., & Randall, R. B.** (2004, November). The application of spectral kurtosis to bearing diagnostics. In *Proceedings of Acoustics* (pp. 3-5).
- [43] **Antoni, J.** (2006). The spectral kurtosis: a useful tool for characterising non-stationary signals. *Mechanical Systems and Signal Processing*, 20(2), 282-307.
- [44] **Antoni, J.** (2007). Fast computation of the kurtogram for the detection of transient faults. *Mechanical Systems and Signal Processing*, 21(1), 108-124.
- [45] **Golub, G. H., & Van Loan, C. F.** (1989). *Matrix computations*, Second ed. John Hopkins University Press.
- [46] **Huang, N. E., Shen, Z., Long, S. R., Wu, M. C., Shih, H. H., Zheng, Q., ... & Liu, H. H.** (1998). The empirical mode decomposition and the Hilbert spectrum for nonlinear and non-stationary time series analysis. *Proceedings of the Royal Society of London. Series A: mathematical, physical and engineering sciences*, 454(1971), 903-995.
- [47] **Moustafa, W., Cousinard, O., Bollaers, F., Sghir, K., & Dron, J. P.** (2016). Low speed bearings fault detection and size estimation using instantaneous angular speed. *Journal of Vibration and Control*, 22(15), 3413-3425.
- [48] **Li, J., Chen, Z., & Li, S.** (2023). Selection of the number of effective singular values for noise reduction. *Mechanical Systems and Signal Processing*, 191, 110175.
- [49] **Kilundu, B., Chimentin, X., & Dehombreux, P.** (2011). Singular spectrum analysis for bearing defect detection. *Journal of Vibration and Acoustics*, vol. 133, no. 5.



CURRICULUM VITAE

Name Surname : Samet Yıldız

EDUCATION :

- **B.Sc.** : 2018, Yıldız Technical University, Mechanical Engineering Faculty, Mechanical Engineering Department

PROFESSIONAL EXPERIENCE AND REWARDS:

- August 2018 - May 2021, BMC POWER Engine and Control Technologies Inc., Mechanical Engineer
- May 2021 - ..., Bosch Sanayi ve Ticaret Anonim Şirketi, Mechanical Engineer
- Awarded best paper of conference, 21st National Machine Theory Symposium, Edirne, Turkey, September 13-15, 2023.

PUBLICATIONS, PRESENTATIONS AND PATENTS ON THE THESIS:

- **Yaldiz S., Sanliturk K.Y.** (2023). Açısal enkoder kullanarak rulman iç bilezik hasar tespiti. *21st National Machine Theory Symposium*, Edirne, Turkey September 13-15.

OTHER PUBLICATIONS, PRESENTATIONS AND PATENTS:

- **Kayaci, N., Demir, H., Yaldiz, S., Eyüp, S., & Tuzcu, C.** (2018). Bina temeline uygulanan toprak kaynaklı ısı pompası sisteminin uzun zamanlı termo-ekonomik optimizasyonu. *4th Anatolian Energy Symposium with International Participation* Edirne, Turkey, April 18-20.